

Isatin-Schiff's base and chalcone hybrids as chemically apoptotic inducers and EGFR inhibitors; design, synthesis, anti-proliferative activities and *in silico* evaluation

Eman A. Fayed^{a,*}, Rogy R. Ezz Eldin^b, Ahmed B.M. Mehany^c, Ashraf H. Bayoumi^d, Yousry A. Ammar^{e,*}

^a Pharmaceutical Organic Chemistry Department, Faculty of Pharmacy (Girls), Al-Azhar University, Nasr City, Cairo, 11754, Egypt

^b Pharmaceutical Organic Chemistry Department, Faculty of Pharmacy, Port Said University, Egypt

^c Zoology Department, Faculty of Science, Al-Azhar University, Nasr City, Cairo 11884, Egypt

^d Pharmaceutical Organic Chemistry Department, Faculty of Pharmacy (Boys), Al-Azhar University, Nasr City, Cairo, 11884, Egypt

^e Chemistry Department, Faculty of Science (Boys), Al-Azhar University, Nasr City, Cairo, 11884, Egypt

ARTICLE INFO

Article history:

Received 13 December 2020

Revised 10 February 2021

Accepted 14 February 2021

Available online 26 February 2021

Keyword:

Indole-2,3-dione schiff's bases

Chalcone

Anti-proliferative activity

Apoptosis

EGFR

ADME properties and molecular docking

ABSTRACT

Isatin derivatives have been found to possess anti-proliferative effects against different human cancer cell lines. A series of isatin-Schiff's base and chalcone were synthesized and screened for their anticancer activities against three human cell lines which are: MCF-7, HepG-2, and HCT-116. All the tested compounds exhibited moderate to high antitumor activity with IC₅₀ ranging from 0.68–35.60 μM compared to Imatinib as a reference standard. Compounds **2b**, **5**, **8b**, **12**, **13a** and **13b** were the most active, with IC₅₀ ranging from 0.68 to 5.85 μM for the three cell lines. The most active structures were selected for further investigations. Firstly, the IC₅₀ values on normal human cells (WI-38) have been studied to ensure the safety of our hits, which showed that our new compounds have exhibited (IC₅₀ > 165.98 μM) as far as their cytotoxic effect is concerned. Moreover, up-regulation of BAX and Caspase-3 and down-regulation of Bcl-2 resulted in the induction of apoptosis from those active compounds. Further work has shown that the most potent derivative **8b**, caused cell cycle arrest at the G2/M phase. Also, EGFR inhibitory activity for **8b** showed IC₅₀ 0.014 μM versus wild EGFR^{WT} and 12.66 nM versus the mutant type, Lapatinib, and Erlotinib were used as reference standards with IC₅₀ values of 0.025, 0.0653 μM and 35.72, 59.56 nM versus both, respectively. Furthermore, the *in-silico* assessment showed that all-potent compounds were orally bioavailable without blood-brain barrier permeation. Finally, the molecular docking of **8b** inside the active site of EGFR (1M17) showed a good binding through three hydrogen bonds and one arene-cation interaction.

© 2021 Elsevier B.V. All rights reserved.

1. Introduction

With the ecological changes and environmental deterioration, cancer has gradually become a major threat to human health [1]. Cancer is one of the degenerative conditions that occur in the age of rodents and humans due to age [2]. Chemotherapy remains among all current therapeutic methods, the most common cancer management options, either alone or in conjunction with surgery and/or radiotherapy [3–5]. One of the best ways to treat cancer is to avoid uncontrolled cancer cell development. The apoptotic approach is thus an exciting way to discover new anti-cancer agents.

In many developmental and physiological environments, apoptosis plays a critical role in monitoring cell numbers. Apoptosis is decreased in several human cancers, which is significantly responsible for transforming the normal cell into tumor cells by disrupting apoptotic function. Apoptosis switching on and off is determined by the relation of BAX proteins and Bcl-2 anti-apoptotic proteins [6]. Two main signaling pathways have been specified for apoptotic cell death, the first being the intrinsic mitochondrial apoptotic pathway, which is primarily produced by cell stress, in which mitochondrial permeability plays a crucial role. The second way is the external cytoplasmic pathway, which is activated via the pro-apoptotic ligands that bind to the death receptor on the cell's surface [7–11].

Caspase protease activity is vital for apoptosis; once active, caspases cleave hundreds of different proteins leading to rapid cell

* Corresponding authors.

E-mail addresses: alfayed_e@azhar.edu.eg (E.A. Fayed), yosry@azhar.edu.eg (Y.A. Ammar).

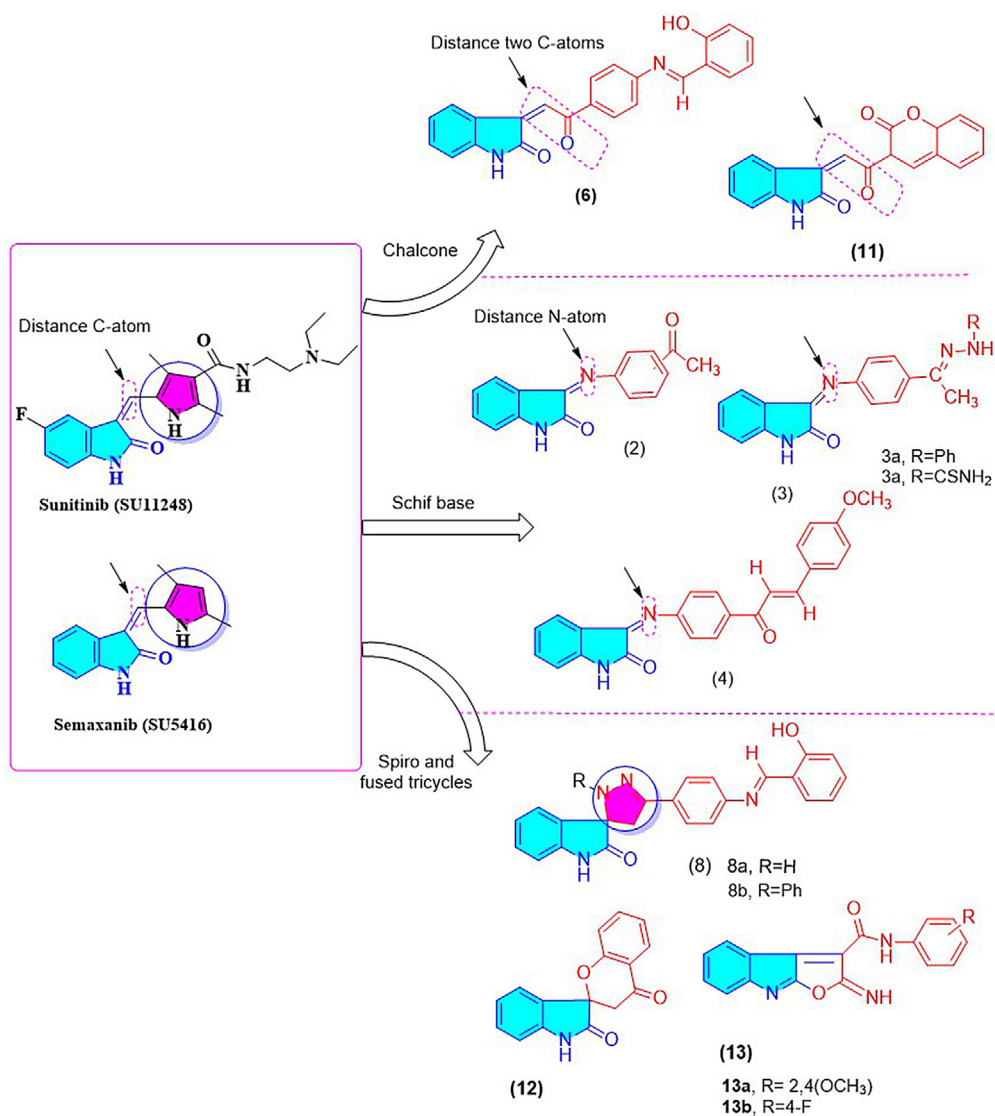


Fig. 1. Structures for some anticancer drugs derived from isatin and the newly synthesized compounds.

death with characteristic biochemical and morphological hallmarks [12–15]. Caspase protease activity is essential to apoptosis; once active, Caspases cluster hundreds of different proteins that result in rapid cell death, with biochemical and morphological characteristics [16,17]. Caspase activity can be initiated either through apoptosis inherent in the pathway or through apoptosis extrinsic pathways. Death of the cells also plays a significant role in cancer therapy. The deregulation of apoptosis has been widely reported as a feature of cancer during cancer disease. Accordingly, apoptosis initiation in tumor cells is an efficient strategy to counter various human malignancies during today's medical age [18–21]. Furthermore, a trans membranous glycope-protein tyrosine kinase receptor is the Epidermal Growth Factor (EGFR) receptor, which is over-expressed by numerous cancer cells, such as (breast, ovarian, human colon) [22]. The over-expression of the EGFR family leads to autophosphorylation of multiple tyrosine residues within the COOH-terminal waist receptor, contributing to a certain storm causing cell proliferation, differentiation, and anti-apoptosis. Therefore, the EGFR family's inhibition has been found to play an important part in the development of targeted chemical-therapeutic agents [23,24]. Currently, in clinical, the anticancer agents suffer from several drawbacks correlated to drugs' associated side effects and/or tumors' multi-drug resistance [25–27]. However, with

the rapidly increasing multidrug-resistance, one of the strategies to overcome this problem is to discover novel molecules with highly potential anticancer activities.

It is well known that isatin is a natural product consisting of many plants, which has also been found to be a common scaffold in various drugs, agrochemicals, and dyes [28–30]. Isatin and its derivatives display diverse pharmacological activities, including antiviral, antitumor, anticonvulsants, antibacterial, and antifungal [31–42]. Some isatin derivatives have been developed as commercial anticancer drugs, such as Sunitinib and Semaxanib (Fig. 1), which identify isatin moiety is an attractive pharmacophore in discovering new drugs [43,44].

Some of the essential techniques for developing new drugs are combining two or more drug-induced compounds in a single molecule to achieve an effect of synergy or to produce new antitumor agents [45–49]. The moieties isatin-chalcone and isatin-Schiff's base have shown potent involvement in antitumor drugs, in addition to the production of spiro-isatin that shows promising antitumor properties. We employed a chalcone and Schiff's base to assemble some novel effective antiproliferative agents in this work. The isatin group is set, and diversity was generated by adding the other rings of various substituents. The target compounds were assessed against cancer cell lines HepG-2, MCF-7 and HCT-116, and

the most active compounds were docked within the active site of EGFR to determine their potential mechanism of action anticancer agents.

2. Experimental

2.1. Chemistry

All melting points were taken on Electrothermal LA 9000 SERIS, Digital Melting point Apparatus, and were uncorrected. IR Spectra were determined using the KBr disk technique on Nicolet IR 200 FT IR Spectrophotometer at Pharmaceutical Analytical Unit, Faculty of Pharmacy, Al-Azhar University, and values are represented in cm^{-1} . The NMR spectra were recorded on Gemini 300 MHz, and Mercury 400 MHz NMR, 75 & 100 for ^{13}C NMR Spectrometer at the Main Chemical Warfare Laboratories, Chemical Warfare Department, Ministry of Defense. DMSO- d_6 was used as a solvent; chemical shifts were measured in δ ppm, relative to TMS as an internal standard. Mass Spectra were recorded at 70 eV on DI-50 unit of Shimadzu GC/MS-QP5050A Spectrometer at Regional Center for Mycology and Biotechnology, Al-Azhar University. Microanalysis was carried out at Regional Center for Mycology and Biotechnology, Al-Azhar University. The anticancer screening was carried out at Regional Center for Mycology and Biotechnology, Al-Azhar University. BAX, Bcl-2, and EGFR, both wild and mutant, were carried out in VACSERA, Cairo, Egypt. The reaction's progress was monitored using TLC sheets pre-coated with UV fluorescent silica gel Merck 60F254 plates and was visualized using a UV lamp. Solvent for TLC: Hexane: Ethyl acetate in ratio 6:4 and 4:6.

3-((3-Acetylphenyl)imino)indolin-2-one & 3-((4-Acetylphenyl)imino)indolin-2-one (2 a,b): were prepared according to the reported method [50,51].

3-((4-(1-(2-Phenylhydrazineylidene)ethyl)phenyl)imino)indolin-2-one (3a)

To a solution of acetophenone derivative **2b** (2.64 g, 0.01 mol) in ethanol/acetic acid (1:1, 20 mL), phenylhydrazine (1.08 mol) was added. The reaction mixture was heated under reflux for 3 h. The solid formed was filtered and crystallized from ethanol.

Brownish powder; Yield: (75%); m.p.: 150–152 °C; IR: ν/cm^{-1} = 3360, 3153 (2NH), 3052 (CH-arom.), 2825 (CH-aliph.), 1682 (C = O), 1600 (C=N); ^1H NMR: δ/ppm = 2.37 (s, 3H, CH_3), 6.53 (d, 2H, J = 9 Hz, Ar-H), 6.85 (d, 4H, J = 9 Hz, Ar-H), 7.05 (t, 1H, Ar-H), 7.24 (t, 2H, Ar-H), 7.47 (d, 1H, J = 6 Hz, Ar-H), 7.50 (d, 2H, J = 9 Hz, Ar-H), 7.64 (d, 1H, J = 6 Hz, Ar-H), 10.98, 12.74 (2 s, 2H, 2NH exchangeable by D_2O); Mass spectrum exhibited a molecular ion peak at m/z : 354.26 (M^+ , 1.14%) with a base peak at m/z : 65.07; Anal. Calc. for $\text{C}_{22}\text{H}_{18}\text{N}_4\text{O}$ (354.41): C, 74.56; H, 5.12; N, 15.81. Found: C, 74.69; H, 5.16; N, 15.93.

2-(1-(4-(2-Oxoindolin-3-ylidene)amino)phenyl)ethylidene)hydrazine-1-carbothioamide (3b)

A solution of acetophenone derivative **2b** (2.64 g, 0.01 mol) in ethanol/acetic acid (1:1, 20 mL) was treated with thiosemicarbazide (0.01 mol). The reaction mixture was heated under reflux for 4 h. The precipitated solid was filtered and crystallized from ethanol.

Brown powder, Yield: (71%); m.p.: 250–252 °C; IR: ν/cm^{-1} = 3422, 3337, 3261, 3169 (NH_2 , 2NH), 3050 (CH-arom.), 2806 (CH-aliph.), 1680 (C = O), 1603 (C = N), 1208 (C = S); ^1H NMR: δ/ppm = 2.49 (s, 3H, CH_3), 6.93 (d, 3H, J = 9 Hz, Ar-H), 7.10 (t, 1H, Ar-H), 7.37 (t, 1H, Ar-H), 7.66 (d, 3H, J = 9 Hz, Ar-H), 8.65, 9.01, 11.17 and 12.46 (4 s, 4H, 2NH and NH_2 exchangeable by D_2O); Mass spectrum exhibited a molecular ion peak at m/z : 337.30 (M^+ , 0.82%) with a base peak at m/z : 40.17. Anal. Calc. for $\text{C}_{17}\text{H}_{15}\text{N}_5\text{OS}$ (337.40): C, 60.52; H, 4.48; N, 20.76. Found: C, 60.84; H, 4.43; N, 20.92.

3-((4-(3-(4-Methoxyphenyl)acryloyl)phenyl)imino)indolin-2-one (4)

To a solution of **2b** (2.64 g, 0.01 mol) and *p*-anisaldehyde (1.24 g, 0.01 mol) in ethanol (20 mL) NaOH (5%, 10 mL) was added. The reaction mixture was stirred for 4 h and left overnight. The precipitated solid was filtered and crystallized from ethanol.

Yellow powder, Yield: (70%); m.p.: 240–242 °C; IR: ν/cm^{-1} = 3261 (NH), 3050 (CH-arom.), 2874 (CH-aliph.), 1742, 1650 (2C=O), 1598 (C = N); ^1H NMR: δ/ppm = 3.82 (s, 3H, OCH_3), 6.36 (d, 2H, J = 6 Hz, Ar-H), 6.71 (t, 1H, Ar-H), 6.89 (d, 2H, J = 6 Hz, Ar-H), 7.01 (d, 2H, J = 6 Hz, Ar-H), 7.08, 7.87 (2d, 2H, J = 16 Hz, CH=CH), 7.14 (d, 2H, J = 6 Hz, Ar-H), 7.33 (t, 1H, Ar-H), 8.26 (d, 2H, J = 6 Hz, Ar-H), 10.98 (s, 1H, NH exchangeable by D_2O); Mass spectrum exhibited a molecular ion peak at m/z : 382.16 (M^+ , 88.3%) with a base peak at m/z : 237.11; Anal. Calc. for $\text{C}_{24}\text{H}_{18}\text{N}_2\text{O}_3$ (382.41): C, 75.38; H, 4.74; N, 7.33. Found: C, 75.52; H, 4.81; N, 7.49.

3-(2-(4-Aminophenyl)-2-oxoethyl)-3-hydroxyindolin-2-one (5) was prepared according to the reported method [52] as

A mixture of isatin (**1**) (1.47 g, 0.01 mol), *p*-aminoacetophenone (1.35 g, 0.01 mol) and diethylamine (3 mL) in ethanol (30 mL), the mixture was stirred for 5 h and left overnight, the obtained product was collected by filtration and crystallized from ethanol.

Pale yellow powder, Yield: (83%); m.p.: 205–207 °C; IR: ν/cm^{-1} = 3437, 3317, 3233 (OH, NH & NH_2), 3058 (CH-arom.), 2914 (CH-aliph.), 1705–1680 (2C=O); ^1H NMR: δ/ppm = 3.43, 3.85 (2d, 2H, J = 18 Hz, CH_2), 5.90 (s, 1H, OH exchangeable by D_2O), 6.03 (s, 2H, NH_2 exchangeable by D_2O), 6.51 (d, 2H, J = 6 Hz, Ar-H), 6.77 (d, 1H, J = 9 Hz, Ar-H), 6.84 (t, 1H, Ar-H), 7.14 (t, 1H, Ar-H), 7.21 (d, 1H, J = 9 Hz, Ar-H), 7.57 (d, 2H, J = 9 Hz, Ar-H), 10.12 (s, 1H, NH exchangeable by D_2O); ^{13}C NMR; 56.46 (CH_2), 73.57 (C_3 -indoline), 112.85, 121.37, 123.84, 124.48, 129.11, 130.72, 131.00, 132.58, 143.45, 154.21 (Ar-Cs), 178.99, 193.68 (2C=O); Mass spectrum exhibited a molecular ion peak at m/z : 282.72 (M^+ , 3.5%) with a base peak at m/z : 83.11; Anal. Calc. for $\text{C}_{16}\text{H}_{14}\text{N}_2\text{O}_3$ (282.30): C, 68.08; H, 5.00; N, 9.92. Found: C, 68.24; H, 4.98; N, 10.08.

3-Hydroxy-3-(2-(4-((2-hydroxybenzylidene)amino)phenyl)-2-oxoethyl)indolin-2-one (6) was prepared according to the reported method [52] as

A mixture of isatin (**1**) (1.47 g, 0.01 mol), 1-(4-((2-hydroxybenzylidene)amino)phenyl)ethanone (0.01 mol) and diethylamine (3 mL) in ethanol (30 mL), the reaction mixture was stirred for 5 h, left for overnight, cooled and treated with ice-cold water, the obtained product was filtered and crystallized from benzene.

Orange powder; Yield: (83%); m.p.: 218–220 °C; IR: ν/cm^{-1} = 3380, 3204 (NH & 2OH), 3059 (CH-Arom.), 2900, 2808 (CH-aliph.), 1695 (2C=O), 1611 (C = N); ^1H NMR: δ/ppm = 3.60, 4.09 (2d, 2H J = 18 Hz, CH_2), 6.03 (s, 1H, OH exchangeable by D_2O), 6.79 (d, 1H J = 6 Hz, Ar-H), 6.85 (d, 1H J = 9 Hz, Ar-H), 6.96 (t, 2H, Ar-H), 7.13 (t, 2H, Ar-H), 7.26 (d, 2H J = 6 Hz, Ar-H), 7.45 (d, 1H J = 9 Hz, Ar-H), 7.68 (d, 1H J = 6 Hz, Ar-H), 7.95 (d, 2H J = 9 Hz, Ar-H), 8.97 (s, 1H, CH=N), 10.23, 12.62 (2 s, 2H, NH & OH exchangeable by D_2O); ^{13}C NMR; 46.18 (CH_2), 73.49 (C_3 -isatin), 109.84, 117.15, 119.78, 121.56, 129.37, 129.98, 132.19, 133.05, 134.68, 134.66, 143.38, 152.99 (Ar-Cs), 160.75 (C = N), 165.35 (C-OH), 178.77, 195.98 (2C=O); Mass spectrum exhibited a molecular ion peak at m/z : 386.12 (M^+ , 1.21%) with a base peak at m/z : 224.06; Anal. Calc. for $\text{C}_{23}\text{H}_{18}\text{N}_2\text{O}_4$ (386.40): C, 71.49; H, 4.70; N, 7.25. Found: C, 71.66; H, 4.81; N, 7.38.

3-(2-(4-((2-Hydroxybenzylidene)amino)phenyl)-2-oxoethylidene)indolin-2-one (7) [52] was prepared by two methods:

First method:

A mixture of 3-hydroxy-indolin-2-one derivative **5** (2.82 g, 0.01 mol), salicylaldehyde (0.01 mol) in ethanol (30 mL) and acetic

acid (3 mL) was heated under reflux for 2 h. The precipitated solid was filtered and crystallized from ethanol.

Second method:

Compound **6** (0.01 mol) in ethanol (30 mL), concentrated HCl (2 mL) was added, the mixture was heated under reflux for 30 min., cooled, and the obtained product was filtered and crystallized from ethanol.

Dark orange powder; Yield: (78%); m.p.: 170–172 °C; IR: ν/cm^{-1} = 3379, 3196 (OH & NH), 3050 (CH-arom.), 2950 (CH-aliph.), 1711 (C=O), 1601 (C = N); $^1\text{H NMR}$: δ/ppm = 6.60 (d, 2H J =6 Hz, Ar-H), 6.73 (d, 2H J =6 Hz, Ar-H), 6.81 (t, 2H, Ar-H), 6.95 (m, 2H, Ar-H), 7.05 (t, 2H, Ar-H), 7.45 (d, 1H J =6 Hz, Ar-H), 7.69 (d, 1H J =6 Hz, Ar-H), 8.32, 8.51 (s, 2H, CH=N), 10.24, 10.67 (2 s, 2H, NH & OH exchangeable by D_2O); $^{13}\text{C NMR}$: 110.56, 117.67, 119.83, 119.92, 120.70, 122.56, 122.73, 125.13, 126.83, 128.89, 129.59, 131.84, 132.35, 133.03, 136.85, 144.64 (Ar-Cs), 155.22 (C = C), 161.17 (C = N), 168.81 (C-OH), 188.39, 192.11 (2C=O); Mass spectrum exhibited a molecular ion peak at m/z : 369.12 (M^+ , 10.19%), 368.10 (M^+ , 32.27%) with a base peak at m/z : 224.06; Anal. Calc. for $\text{C}_{23}\text{H}_{16}\text{N}_2\text{O}_3$ (368.38): C, 74.99; H, 4.38; N, 7.60. Found: C, 75.12; H, 4.42; N, 7.69.

5'-(4-((2-Hydroxybenzylidene)amino)phenyl)-4'-hydrospiro(indoline-3,3'-pyrazol)-2-one (8a,b):

A mixture of isatin derivative **7** (3.69 g, 0.01 mol) and hydrazine hydrate or phenylhydrazine (0.012 mol) in ethanol (20 mL) containing acetic acid (5 mL) was heated under reflux for 7 h, cooled, and the obtained product was filtered and crystallized from ethanol.

5'-(4-((2-Hydroxybenzylidene)amino)phenyl)-2',4'-dihydrospiro(indoline-3,3'-pyrazol)-2-one (8a)

Brown powder, Yield: (83%); m.p.: 220–222 °C; IR: ν/cm^{-1} = 3337, 3262, 3169 (OH & 2 NH), 3025 (CH-arom.), 2996 (CH-aliph.), 1668 (C = O), 1598 (C = N); $^1\text{H NMR}$: δ/ppm = 3.60, 3.85 (2d, 2H, J =18 Hz, CH_2), 5.62, (1 s, 1H, 1NH exchangeable by D_2O), 6.72 (d, 1H J = 6 Hz, Ar-H), 6.78 (d, 2H J = 6 Hz, Ar-H), 6.84 (m, 1H, Ar-H), 6.87 (t, 2H, Ar-H), 7.11 (t, 2H, Ar-H), 7.28 (d, 2H, Ar-H), 7.52 (d, 1H J = 6 Hz, Ar-H), 7.71 (d, 1H J = 6 Hz, Ar-H), 8.36 (s, 1H, CH=N), 11.10, 12.49 (2 s, 2H, OH & 1NH exchangeable by D_2O); $^{13}\text{C NMR}$ (101 MHz, DMSO) δ 43.80 (CH_2), 67.95 (C-spiro), 111.42, 115.76, 119.48, 121.15, 122.30, 123.50, 124.67, 125.87, 127.54, 129.98, 131.95, 133.93, 135.59, 140.46, 143.50, 151.60, 154.59, 157.76, 161.57 (2 C=N), 165.28 (C-OH), 168.61(C=O); Mass spectrum exhibited a molecular ion peak at m/z : 382.24 (M^+ , 2.18%) with a base peak at m/z : 120.09; Anal. Calc. for $\text{C}_{23}\text{H}_{18}\text{N}_4\text{O}_2$ (382.41): C, 72.24; H, 4.74; N, 14.65. Found: C, 72.39; H, 4.79; N, 14.78.

5'-(4-((2-Hydroxybenzylidene)amino)phenyl)-2'-phenyl-2',4'-dihydrospiro[indoline-3,3'-pyrazol-ol]-2-one (8b)

Deep orange powder; Yield: (71%); m.p.: 120–122°C; IR: ν/cm^{-1} = 3370, 3310 (OH & NH), 3038 (CH-arom.), 2822 (CH-aliph.), 1680 (C=O), 1597 (C=N); $^1\text{H NMR}$: δ/ppm = 3.24, 3.35 (2d, 2H, J = 18 Hz, CH_2), 6.73 (t, 2H, Ar-H), 6.85 (d, 2H, J =9 Hz, Ar-H), 6.96 (d, 1H, J =6 Hz, Ar-H), 7.13 (d, 2H, J =6 Hz, Ar-H), 7.20 (t, 2H, Ar-H), 7.36–7.43 (m, 6H, Ar-H), 7.53 (d, 2H, J =9 Hz, Ar-H), 8.23 (s, 1H, CH=N), 10.37, 10.55 (2 s, 2H, OH & NH exchangeable by D_2O); $^{13}\text{C NMR}$ (101 MHz, DMSO) δ 45.06 (CH_2), 66.42 (C-spiro), 111.52, 114.67, 116.32, 118.79, 121.22, 123.26, 124.84, 125.90, 128.20, 130.00, 132.02, 133.75, 134.92, 136.59, 138.09, 141.00, 142.13, 143.68, 147.57, 149.15, 151.79, 155.70, 160.92 (2 C=N), 165.94 (C-OH), 169.46 (C=O); Mass spectrum exhibited a molecular ion peak at m/z : 458.13 (M^+ , 0.88%) with a base peak at m/z : 44.03; Anal. Calc. for $\text{C}_{29}\text{H}_{22}\text{N}_4\text{O}_2$ (458.52): C, 75.97; H, 4.84; N, 12.22. Found: C, 76.12; H, 4.91; N, 12.34.

1-(4-(2-(3-Hydroxy-2-oxoindolin-3-yl)acetyl)phenyl)-3-phenylthiourea (9)

A mixture of isatin (**1**) (1.47 g, 0.01 mol), the corresponding thiourea derivative (2.70 g, 0.01 mol) and diethylamine (3 mL) in ethanol (30 mL), the mixture was stirred for 5 h, left overnight, cooled, and the obtained product was filtered and crystallized from ethanol.

Yellowish powder; Yield: (82%); m.p.: 185–187°C; IR: ν/cm^{-1} = 3425, 3216 (OH, 3NH), 3031 (CH-arom.), 1705, 1666 (2C=O), 1328 (C=S); $^1\text{H NMR}$: δ/ppm = 3.51, 4.00 (2d, 2H, J =12 Hz, CH_2), 6.00 (s, 1H, OH exchangeable by D_2O), 6.47 (d, 1H, J =8 Hz, Ar-H), 6.52 (t, 1H, Ar-H), 6.73 (t, 1H, Ar-H), 6.78 (t, 1H, Ar-H), 7.17 (d, 1H, J =8 Hz, Ar-H), 7.42 (t, 2H, Ar-H), 7.62 (d, 2H, J =8 Hz, Ar-H), 7.81 (d, 2H, J =8 Hz, Ar-H), 7.91 (d, 2H, J =8 Hz, Ar-H), 9.75, 10.09, 10.20 (3 s, 3H, 3NH exchangeable by D_2O); Mass spectrum exhibited a molecular ion peak at m/z : 417.31 (M^+ , 0.81%) with a base peak at m/z : 77.07; Anal. Calc. for $\text{C}_{23}\text{H}_{19}\text{N}_3\text{O}_3\text{S}$ (417.48): C, 66.17; H, 4.59; N, 10.07. Found: C, 66.40; H, 4.63; N, 10.29.

N-(4-(2-(3-Hydroxy-2-oxoindolin-3-yl)acetyl)phenyl)-4-methylbenzenesulfonamide (10)

A mixture of isatin (**1**) (1.47 g, 0.01 mol), the corresponding acetyl sulfonamide derivative (2.89 g, 0.01 mol) and diethylamine (3 mL) in ethanol (30 mL), the mixture was stirred for 5 h, left overnight, cooled, and the obtained product was filtered and crystallized from ethanol.

Yellowish powder; Yield: (78%); m.p.: 165–167°C; IR: ν/cm^{-1} = 3454, 3218 (br. OH & 2NH), 3050 (CH-arom.), 2938 (CH-aliph.), 1720, 1668 (2C=O); $^1\text{H NMR}$: δ/ppm = 2.31 (s, 3H, CH_3), 3.39, 3.98 (2d, 2H, J =12 Hz, CH_2), 6.00 (s, 1H, OH exchangeable by D_2O), 6.73 (d, 1H, J =8 Hz, Ar-H), 6.78 (t, 1H, Ar-H), 7.12 (d, 1H, J =8 Hz, Ar-H), 7.16 (d, 2H, J =8 Hz, Ar-H), 7.33 (d, 2H, J =8 Hz, Ar-H), 7.66 (t, 1H, Ar-H), 7.71 (d, 2H, J =8 Hz, Ar-H), 7.79 (d, 2H, J =8 Hz, Ar-H), 10.19, 10.73 (2 s, 2H, 2NH exchangeable by D_2O); $^{13}\text{C NMR}$: 26.55 (CH_3), 56.50 (CH_2), 80.00 (C3-indolinone), 106.03, 116.52, 116.59, 117.42, 117.67, 118.52, 119.52, 121.60, 123.77, 128.33, 128.40, 129.48, 142.37, 145.09 (Ar-Cs), 162.01, 162.10 (2C=O); Mass spectrum exhibited a molecular ion peak at m/z : 436.30 (M^+ , 2.24%) with a base peak at m/z : 91.08; Anal. Calc. for $\text{C}_{23}\text{H}_{20}\text{N}_2\text{O}_5\text{S}$ (436.11): C, 63.29; H, 4.62; N, 6.42. Found: C, 63.42; H, 4.68; N, 6.65.

3-(2-Oxo-2-(2-oxo-2H-chromen-3-yl)ethylidene)indolin-2-one (11) [53,54]

A mixture of isatin (**1**) (1.47 g, 0.01 mol), acetyl coumarin (1.90 g, 0.01 mol) and diethylamine (3 mL) in ethanol (30 mL), the mixture was stirred for 5 h, left overnight, cooled, and the obtained product was filtered and crystallized from ethanol.

Pale yellow powder; Yield: (73%); m.p.: 250–252°C; IR: ν/cm^{-1} = 3428 (NH), 3112 (CH-arom.), 1717–1645 (3C=O); $^1\text{H NMR}$: δ/ppm = 7.47 (s, 1H, CH-ethylinic), 7.52 (d, 1H, J =6 Hz, Ar-H), 7.59 (d, 1H, J =6 Hz, Ar-H), 7.67 (d, 2H, J =6 Hz, Ar-H), 7.84 (t, 2H, Ar-H), 8.22 (t, 2H, Ar-H), 8.39 (s, 1H, CH-coumarin), 11.09 (1 s, 1H, NH exchangeable by D_2O); $^{13}\text{C NMR}$: 113.45, 121.94, 125.55, 126.08, 127.53, 128.30, 128.39, 128.53, 129.41, 130.61, 134.55, 135.65, 141.13 (Ar-Cs), 146.06, 155.37 (C=C), 161.55 (C-O), 161.69, 163.74, 172.36 (3C=O); Mass spectrum exhibited a molecular ion peak at m/z : 317.12 (M^+ , 1.57%) with a base peak at m/z : 156.21; Anal. Calc. for $\text{C}_{19}\text{H}_{11}\text{NO}_4$ (317.30): C, 71.92; H, 3.49; N, 4.41. Found: C, 71.75; H, 3.69; N, 4.18.

Spiro[chroman-2,3'-indoline]-2',4'-dione (12)

A solution of isatin(**1**)(1.47 g, 0.01 mol), 2-hydroxyacetophenone (1.38 g, 0.01 mol) in ethanol (30 mL), was treated with diethylamine (3 mL), the mixture was stirred for 5 h, left overnight, cooled and the obtained product was filtered and crystallized from ethanol.

Orange powder; Yield: (83%); m.p.: 240–242°C; IR: ν/cm^{-1} = 3418 (NH), 3050 (CH-arom.), 2992, 2805 (CH-aliph.), 1655 (br 2C=O); $^1\text{H NMR}$: δ/ppm = 3.45, 3.97 (2d, 2H, J =8 Hz,

CH₂), 6.73 (d, 1H, J=6 Hz, Ar-H), 6.82 (t, 2H, Ar-H), 6.90 (d, 1H, J=6 Hz, Ar-H), 7.47 (t, 2H, Ar-H), 7.60 (d, 2H, J=9 Hz, Ar-H), 10.39 (s, 1H, NH exchangeable by D₂O); ¹³C NMR: 56.05 (CH₂), 113.46 (C3-indoline), 114.50, 122.37, 125.59, 126.12, 127.52, 128.31, 130.64, 131.39, 141.16, 142.93, 146.05 (Ar-Cs), 155.62 (C=O), 163.70, 187.84 (2C=O); Mass spectrum exhibited a molecular ion peak at m/z: 265.16 (M⁺, 2.72%) with a base peak at m/z: 76.07; Anal. Calc. for C₁₆H₁₁NO₃ (265.26): C, 72.45; H, 4.18; N, 5.28. Found: C, 72.68; H, 4.22; N, 5.43.

N-(Aryl)-2-imino-2H-furo[2,3-b]indole-3-carboxamides (13a, b):

To a solution of isatin (**1**) (1.47 g, 0.01 mol) in ethanol (30 mL), cyanoacetranilide derivatives (0.01 mol) and piperidine (0.5 mL) were added. The reaction mixture was heated under reflux for 3 h, left overnight, cooled, and the obtained product was filtered and crystallized from ethanol.

N-(2,4-Dimethoxyphenyl)-2-imino-2H-furo[2,3-b]indole-3-carboxamide (13a):

Reddish brown powder; Yield: (66%); m.p.: 165–167 °C; IR: ν/cm^{-1} = 3423, 3365 (br 2NH), 3050 (CH-arom.), 2942, 2842 (CH-aliph.), 1660 (C=O), 1613 (2C=N); ¹H NMR: δ/ppm = 3.60, 3.67 (2 s, 6H, 2OCH₃), 6.48 (d, 1H, J=6 Hz, Ar-H), 6.70 (s, 1H, Ar-H), 6.93 (t, 1H, Ar-H), 6.82 (d, 1H, J=9 Hz, Ar-H), 7.30 (t, 1H, Ar-H), 8.22 (d, 1H, J=6 Hz, Ar-H), 9.04 (d, 1H, J=6 Hz, Ar-H), 10.98, 11.52 (2 s, 2H, 2NH exchangeable by D₂O); Mass spectrum exhibited a molecular ion peak at m/z: 349.62 (M⁺, 4.30%) with a base peak at m/z: 138.12; Anal. Calc. for C₁₉H₁₅N₃O₄ (349.35): C, 65.32; H, 4.33; N, 12.03. Found: C, 65.12; H, 4.94; N, 12.21.

N-(4-Fluorophenyl)-2-imino-2H-furo[2,3-b]indole-3-carboxamide (13b):

Dark red powder; Yield: (67%); m.p.: 300–302 °C; IR: ν/cm^{-1} = 3224 (2NH), 3050 (CH-arom.), 2815 (CH-aliph.), 1665 (C=O), 1612 (2C=N); ¹H NMR: δ/ppm = 6.93 (d, 2H, J=6 Hz, Ar-H), 7.12 (t, 1H, Ar-H), 7.58 (d, 1H, J=6 Hz, Ar-H), 7.45 (t, 1H, indolin-5), 7.61 (d, 1H, J=6 Hz, Ar-H), 7.93 (d, 2H, J=9 Hz, Ar-H), 10.88, 10.99 (2 s, 2H, 2NH exchangeable by D₂O); ¹³C NMR: 108.76, 111.57, 115.07, 116.21, 119.45, 122.36, 123.03, 124.26, 125.58, 134.39, 140.81 (Ar-Cs), 144.85, 145.40 (2C=C), 158.21, 158.54 (2C=N), 158.83 (C-F), 165.51 (C=O); Mass spectrum exhibited a molecular ion peak at m/z: 307.15 (M⁺, 2.03%) with a base peak at m/z: 111.10; Anal. Calc. for C₁₇H₁₀FN₃O₂ (307.28): C, 66.45; H, 3.28; N, 13.67. Found: C, 66.67; H, 3.26; N, 13.

2.2. Biological activities

2.2.1. Cell lines

Human breast (MCF-7), hepatocellular (Hep-G2), and colon (HCT-116) carcinoma cells were obtained from the American Type Culture Collection (ATCC, Rockville, MD, USA). The cells grown in RPMI-1640 medium, supplemented with 10% inactivated fetal calf serum and 50 µg/mL gentamycin. The cells were maintained at 37°C in a humidified atmosphere with 5% CO₂.

2.2.2. Evaluation of the antitumor activity by MTT assay

Viability of control and treated cells were evaluated using the MTT assay in triplicate. The MTT assay is a laboratory test and a standard colorimetric assay (an assay which measures color changes) for measuring cellular growth, Yellow MTT (3-(4,5-dimethylthiazol-2-yl)-2,5-diphenyl tetrazolium bromide, a tetrazole) was reduced to purple formazan in the mitochondria of living cells. A solubilization solution (dimethyl sulfoxide) was added to dissolve the insoluble purple formazan product into a colored solution. Briefly, three tumor cell lines were seeded in 96-well plates containing 100 µL of the growth medium at a density of 1×10^4 cells/well. Cells were permitted to adhere for 24 h till

confluence, washed with PBS, and then treated with different concentrations of compounds in fresh maintenance medium from 50 to 1.56 µg and incubated at 37 °C for 24 h. Control of the untreated cells was made in the absence of the test compound. The untreated cells were used as negative control. Serial two-fold dilutions of the tested compounds were added into a 96-well tissue culture plate using a multichannel pipette (Eppendorf, Germany). After treatment (24 h), the culture supernatant was replaced by fresh medium. Then, the cells in each well were incubated at 37°C with 100 µL of MTT solution (5 mg/mL) for 4 h. After incubation, the MTT solution was removed, and then 100 µL of DMSO was added to each well. The absorbance was detected at 570 nm using a microplate reader (Sun Rise TECAN, Inc, USA). The absorbance of untreated cells was considered as 100%. The results were determined by three independent experiments [55].

2.2.2.1. Data analysis. The percentage of cell viability was calculated as follows = $[1 - (\text{ODt}/\text{ODc})] \times 100\%$, where ODt is the mean optical density of wells treated with the tested compound and ODc is the mean optical density of untreated cells. The tested compounds were compared using the IC₅₀ value, i.e., the concentration of an individual compound leading to 50% cell death estimated from graphical plots of surviving cells verses compound concentrations.

2.2.3. Apoptosis detection studies

2.2.3.1. Determination of the active caspase-3. The manufacturer's protocol calculated the active level of Caspase-3 with an active Quantikine-Human Caspase-3 Immunoassay (R&D Systems, Inc. Minneapolis, USA). After cell washing with PBS, the cells were collected and lysed by adding them to the protease inhibitor extraction buffer (1 mL per 1×10^7 cell). The lysate was diluted immediately before the test. Finally, a microplate reader set at 450 nm calculated the optical density of each well in 30 min [46].

2.2.3.2. Determination of mitochondrial apoptosis pathway proteins BAX and Bcl-2. Cells were extracted from the American Culture Set, cells were grown in RPMI 1640 containing 10% fetal serum from bovine animals at 37°C, the compounds were stimulated for the BAX or Bcl-2 test, and the cell extraction buffer was lysed. This lysate was diluted across the test range and tested for human active BAX or Bcl-2 content in Regular Diluent Buffer. (Cells are Plated in the density of $1.2 - 1.8 \times 10,000$ cells/well in a volume of 100 µL complete growth medium + 100 uL of the tested compound per well in a 96-well plate for 24 h before measuring for human active BAX or Bcl-2) [6].

2.2.4. Cell cycle analysis

The MCF-7 cancer cells were seeded into a 6-well plate and incubated for 24 h at a concentration of 1×10^5 cells per well. Cells have been treated with a vehicle (0.1 percent DMSO) or with a compound **8b** for 24 h. Afterward, cells were harvested with ice-cold 70% ethanol at 4 °C and fixed for 12 h. Ethanol and cold PBS are extracted from the cells and incubated in 0.5 mL P BS containing 1 mg/mL Rnase for 30 min. at a temperature of 37°C. The cells were stained with propidium iodide in the dark for about 30 min. The DNA contents were then measured by the flow cytometer [56].

2.2.5. Annexin v-FITC assay

The MCF-7 cancer cells have been plated in a 6-well plate, incubated for 24 h, then treated in a vehicle (0.1% DMSO) or compound **8b** for 24 h. The binding buffer (10 mM HEPES, 140 mM NaCl, and 2.5 mM CaCl₂ at pH 7.4) was used to harvest cells, wash them with PBS and spray them in the dark with Annexin V-FITC and propidium iodide (PI). The flow cytometer was then analyzed [57–59].

2.2.6. EGFR assay

Inhibitory behavior of the most promising compound **8b** on the MCF-7 cells was carried with the same instructions and the recorded method against EGFR^{wt} and EGFR^{L858R-TK} from the protocol producer [23,24].

2.2.7. In silico physicochemical and ADME properties prediction

Using Chemdraw 12.0, the molecular structures have been converted to SMILES. Such SMILES were then introduced into the Swiss ADME website for the purposes of measuring physicochemical descriptors, lipophilicity, pharmacokinetics, ADME parameters, and medicinal chemistry friendliness [60].

2.2.8. Molecular docking

Molecular modeling was carried out using Molecular Operating Environment software 10.2008 (MOE), Chemical Computing Group Inc., Montreal, Quebec, Canada, as the computational software and docking process performed as described in previous work [23]. The enzyme (**1M17**) [24] was downloaded from the protein data bank, water molecule removed, all hydrogen atom was added, then refined, and energy minimized were performed with MOE. The validation process was performed by redocking the Erlotinib into the EGFR binding site using the MOE software default set to confirm that the protein is ready for docking. The target compound was drawn in chem draw then transferred to MOE where protonated 3D, render hidden hydrogen and finally, energy minimized and saved as mdb for docking inside active site. Then, the docking process was performed using the default protocol.

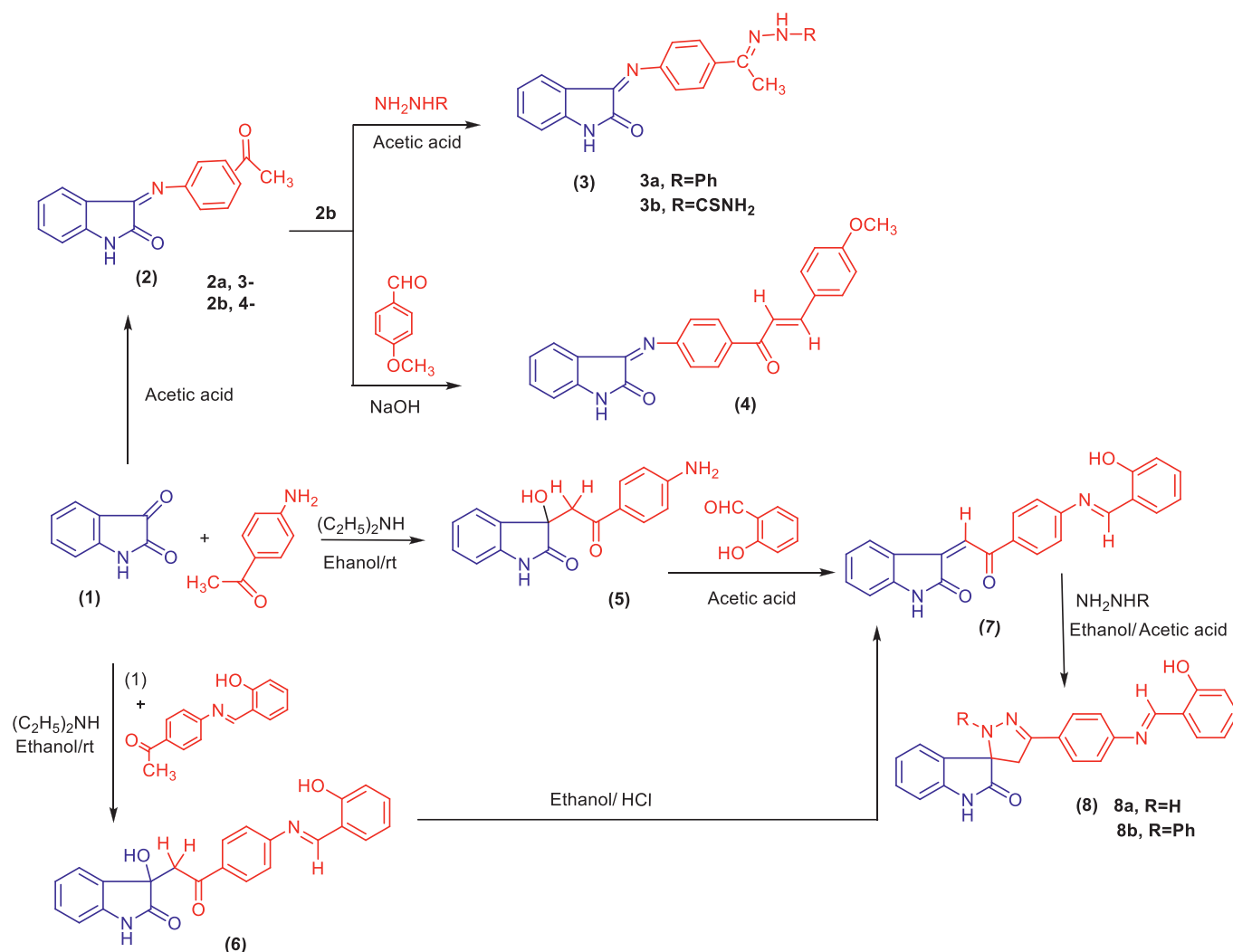
3. Results and discussion

3.1. Chemistry

In continuation of our work to synthesize some heterocyclic compounds in the field of medicinal chemistry [61–66], it seemed of interest to design and synthesize a novel series of isatin derivatives bearing biologically active units to evaluate their anti-cancer activity. Preparation of the isatin derivatives is outlined in **schemes 1&2**. The behavior of isatin (**1**) with aminoacetophenone derivatives was discussed. The aminoacetophenone has two nucleophilic centers; thus, its reaction with isatin dependent on the reaction conditions. Condensation of *p*-aminoacetophenone with isatin in acetic acid afforded Schiff's base product, which was identified as 3-((3 or 4-acetylphenyl)imino)indolin-2-one (**2a,b**), where the condensation occurred through the amino group that prepared according to reported methods [50,51]. The resulting Schiff base **2b** has acetyl function, which was subjected to react with phenylhydrazine, thiosemicarbazide, or anisaldehyde to afford a single product in each case. The product formed was formulated as the phenylhydrazone, thiosemicarbazone, and unsaturated ketone derivatives **3–4**, respectively. The structure of these products **3a, b**, and **4** was confirmed based on their correct elemental analyses and spectral data. The IR spectra of **3a** showed two NH stretching bands at ν 3360, 3153 cm^{-1} , the carbonyl function was observed at 1682. The ^1H NMR spectra of **3b** displayed a singlet signal at δ 2.49 ppm due to CH_3 , with four singlet signals related to NH & NH_2 protons of the thiosemicarbazone moiety and NH indole at δ 8.65, 9.01, 11.17, and 12.46 ppm, which all exchanged by D_2O . The aromatic protons were observed as a multiplet at δ 6.93–7.66 ppm integrated for (8H) protons. ^1H NMR spectral data of unsaturated ketone with 2-oxo-indole derivative **4** showed a singlet signal at δ 3.82 ppm due to methoxy group, and a singlet at δ 10.98 ppm indicating the presence of NH. Besides, the protons of α,β -unsaturated system that observed as two doublets around δ 7.08, ppm for H-

α and 7.87 ppm for H- β with coupling constant ($J=15$ Hz), which indicated the trans isomer.

On the other hand, aldol condensation of *p*-aminoacetophenone with isatin in absolute ethanol in the presence of few drops of *N,N*-diethylamine (DEA) as a catalyst, the final product separated and identified as 3-(2-(4-aminophenyl)-2-oxoethyl)-3-hydroxyindolin-2-one (**5**). The structure of product **5** was ascertained from their spectral features. The IR spectrum of compound **5** showed absorption bands at ν 3437, 3317, and 3233 cm^{-1} assignable to OH, NH_2 , and NH groups, and a band at ν 1705–1680 cm^{-1} due to two carbonyl functions. Its ^1H NMR spectrum showed two doublets singlet at δ 3.43, 3.85 ppm corresponding for CH_2 protons. Three singlet signals were observed at δ 5.9, 6.03, and 10.12 ppm for OH, NH_2 , and NH, respectively. The phenyl protons appeared in addition to the indoline doublets and triplet signals between δ 6.51–7.57 ppm for eight protons. Typical ^{13}C NMR spectrum displayed signals for CH_2 and C_3 -indoline carbon at 56.45 and 73.57 besides aromatic carbon in the region of δ 112.85–154.21 ppm, and carbonyl carbons appeared at δ 178.99 and 193.68 ppm. Condensation of compound **5** with salicylaldehyde afforded a product that was formulated as the corresponding Schiff's base **7**, and dehydration occurred. This compound was confirmed chemically by another way where the reaction of isatin with 1-(4-(2-hydroxybenzylidene)amino)phenyl)ethanone to furnish the 3-hydroxy-3-substituted-2-oxoindole derivative **6** which exposed to dehydration with ethanolic hydrochloric. Unfortunately, both elemental analysis and spectral data of the 3-hydroxyl 2-oxo-indole derivatives **6** and Schiff's base **7** were on assignment with the possible structures. The structure of product **6** was confirmed from their spectral features. The IR revealed two hydroxy (OH) and NH groups as a broad band around at ν 3380, 3204 cm^{-1} and two carbonyl groups at ν 1695 cm^{-1} . ^1H NMR spectrum ($\text{DMSO}-d_6$) exhibited two doublets at δ 3.60, 4.09 ppm assignable to CH_2 protons, other three singlet signals at δ 6.03, 10.23, 12.62 ppm due to two hydroxy and NH protons, the aromatic protons were observed as multiplet signals at δ 6.79–7.95 ppm. Also, ^{13}C NMR exhibited three signals at δ 46.18, 73.49 ppm due to CH_2 and C_3 -indoline besides Ar-Cs at δ 109.84–152.99 ppm and two signals a δ 160.75, 165.35 ppm for (C=N) and (C-OH) respectively, and two C=O at δ 178.77 and 195.98 ppm. The mass spectrum showed a molecular ion peak at $m/z = 386$, corresponding to a molecular formula $\text{C}_{23}\text{H}_{18}\text{N}_2\text{O}_4$. The structure of compound **7** was confirmed on the basis of its spectral data; its IR spectrum showed absorption bands at ν 3379, 3196 cm^{-1} assignable to OH and NH groups, and a band at ν 1711 cm^{-1} due to C=O function in addition to the band at ν 1601 cm^{-1} corresponding for C=N. ^1H NMR spectrum showed two singlet signals were observed at δ 10.24, 10.67 ppm for OH, and NH respectively, the aromatic protons have appeared at range δ 6.60–7.91 ppm. ^{13}C NMR spectrum displayed signals for aromatic carbons & C=C in the region of δ 110.56–155.22 ppm, and carbonyl carbons appeared at δ 188.39 and 192.11 ppm. Cyclo-condensation of α, β -unsaturated ketone **7** with hydrazine or phenylhydrazine was carried out in ethanol containing acetic acid and afforded spiropyrazoline derivatives **8a,b** (**Scheme 1**). Compound **8a,b** was suggested for the reaction product based on both elemental and spectral analyses. The IR spectrum of **8a** as an example showed intense peaks at ν 3337, 3262, 3169 cm^{-1} for OH and NH groups, respectively, in addition to absorption peak at ν 1668 cm^{-1} for carbonyl (C=O) and ν 1598 cm^{-1} for (C=N) stretching. Its ^1H NMR spectrum showed two doublet signal at δ 3.60, 3.85 ppm due to CH_2 , a multiplet at δ 6.72–7.71 ppm was observed for the aromatic twelve protons, a singlet was observed at δ 8.36 ppm due to CH=N. Besides, three D_2O -exchangeable signals at δ 5.62, 11.10, 12.49 ppm due to two NH and phenolic hydroxyl groups. ^{13}C NMR showed signal at δ 43.80 ppm due to CH_2 , 67.95 for sipro carbon (C3-indoline), and two signals at δ 157.76 and 161.57 ppm for two

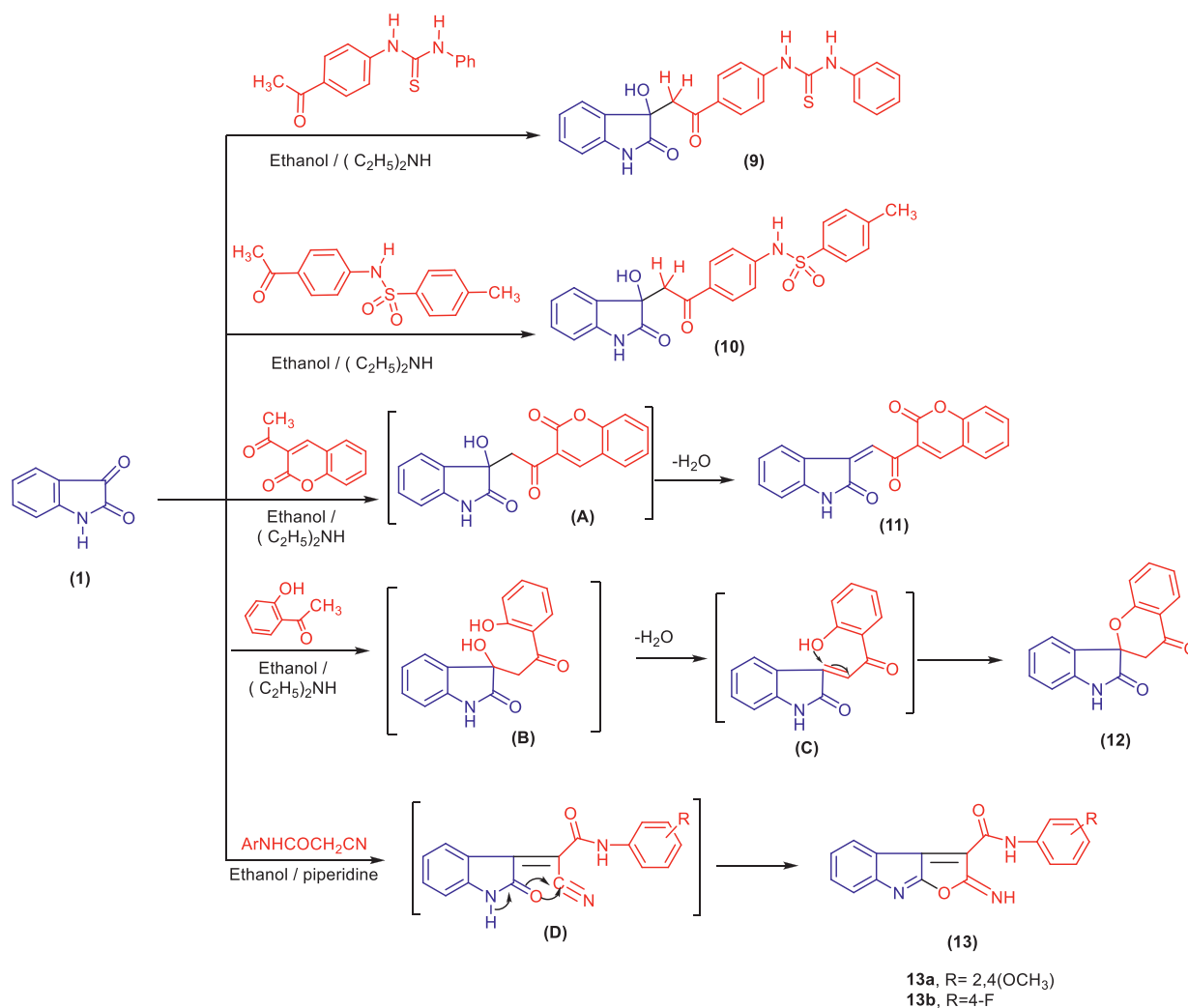


2C=N as well as two significant signals at δ 165.28, 168.61 ppm for carbon attached for hydroxy and carbonyl groups, besides the aromatic-carbons.

In continuation of this investigation, another type of acetyl derivative was used as reagents to react with isatin in the hope of obtaining more pharmacologically active compounds. Thus, reaction of isatin (1) with 1-(4-acetylphenyl)-3-phenylthiourea furnished a product was formulated as 1-(4-(2-(3-hydroxy-2-oxindolin-3-yl)acetyl)-phenyl)-3-phenylthiourea (9). The structure of the compound 9 was elucidated based on their spectral data and elemental analyses. Its IR spectra revealed absorption bands at ν 3425, 3216 cm^{-1} assignable to OH and three NH groups and absorption bands at 1705 and 1666 due to C=O groups, 1328 due to C=S. The ^1H NMR spectrum of compound 9 exhibited two doublet signals at δ 3.51 and 4.00 ppm representing the protons of methylene group (CH_2) and four exchangeable D_2O signals at δ 6.00, 9.75, 10.09 and 10.20 ppm for OH and three NH groups, besides aromatic protons which observed in the region δ 6.47–7.93 ppm. Its mass spectrum showed a peak corresponding to the molecular ion at m/z 417 (0.81%) with a base peak at m/z 77. Also, the interaction of isatin (1) with *N*-(4-acetylphenyl)-4-methylbenzenesulfonamide in the presence of diethylamine, the 3-hydroxy 2-oxindole derivative was obtained and identified as *N*-(4-(2-(3-hydroxy-2-oxindolin-3-yl)acetyl)phenyl)-4-methylbenzenesulfonamide (10). The struc-

ture of compound 10 was deduced based on their spectral data and elemental analyses. The IR spectrum of compound 10 revealed an absorption band at ν 3454, 3218 cm^{-1} due to OH and two NH groups, and absorption bands at ν 1668, 1720, and 1597 attributed to two C=O and C=N respectively. Its ^1H NMR spectrum showed a singlet at δ 2.31 ppm assigned to the CH_3 protons and the presence of the CH_2 protons at δ 3.44, 3.98 ppm that confirmed the structure. Also, a multiplet in the region of δ 6.73–7.79 ppm due to aromatic protons besides two D_2O exchangeable signals at δ 10.09, 10.73 ppm assigned to 2 NH. ^{13}C NMR showed a signal at 26.55 ppm attributed to CH_3 , methylene carbon at δ 56.50 ppm, and two signals at δ 162.01 and 162.10 ppm due to two carbonyl carbons besides the aromatic carbons.

On the other hand, 3-(2-oxo-2-(2-oxo-2H-chromen-3-yl)ethylidene)indolin-2-one (11) was obtained upon treatment isatin (1) with 3-acetyl-2H-chromen-2-one in the presence of diethylamine. The reaction proceeded via acetyl group's addition to afford the intermediate, which was subjected to dehydration under the reaction condition. The structure of compound 11 was deduced on the basis of their elemental analyses and spectral data. Its IR spectrum of the compound revealed an absorption band at ν 3428 cm^{-1} due to NH and three carbonyl groups observed at ν 1645–1717 cm^{-1} . Its ^1H NMR spectrum exhibited signals around δ 7.47–8.39 ppm attributed aromatic protons, CH=ethylinic, and 4-H coumarin. Its ^{13}C NMR displayed three carbonyl carbons at δ



Scheme 2. synthesis of compounds 9–13.

161.69, 163.74, and δ 172.36 ppm besides the aromatic carbons. The mass spectrum showed a molecular ion peak at m/z 317 (1.57%) with a base peak at m/z 156.

Furthermore, spiro[chroman-2,3'-indoline]-2',4dione (**12**) was prepared in one step on the reaction of isatin **1** with 2-hydroxyacetophenone in the presence of diethylamine as a catalyst. The structure of **12** was established based on elemental and spectral data. Its IR spectrum revealed the presence of an absorption band at ν 3418 cm^{-1} due to NH, and two carbonyl groups observed at 1653 cm^{-1} . The ^1H NMR spectrum revealed singlet signal at δ 3.45 attributable to CH_2 in addition to the aromatic protons and D_2O exchangeable proton at δ 10.39 ppm related to NH of isatin derivatives. Also, ^{13}C NMR revealed a signal at δ 56.05 ppm due to CH_2 and three signals at δ 113.46, 163.70 and 187.84 ppm assigned to spirocarbon (C3-indoline) and two carbonyl carbons besides the aromatic carbons that ranged between δ 114.50 to 146.05 ppm. The formation of compound **12** is assumed to proceed via the formation of unsaturated ketone (intermediate **B** subjected to hydration). Then, the hydroxyl group present in the ortho position of acetophenone acts as nucleophilic addition on alkene double bond through intramolecular cyclization (intermediate **C**) to afford the final product.

Finally, isatin was subjected to react with cyano acetanilide derivatives as an active methylene compound, and the actual structure of the product was assigned as *N*-(substitutedphenyl)-2-

imino-2*H*-furo[2,3-*b*]indole-3-carboxamides (**13a, b**) based on the elemental analyses and the spectral data. The formation of compound **13a, b** is assumed to proceed via the nucleophilic addition of the active methylene in the cyano acetanilide derivatives to the carbonyl group of isatin in position three followed by dehydration to afford the arylidene intermediate **D**, which underwent nucleophilic attack of the hydroxyl group to the nitrile function to give the final product. The IR spectrum of **13a** revealed the lack of nitrile band and the presence of absorption bands at ν 3423 and 1660 cm^{-1} due to 2 NH, and carbonyl groups, respectively. ^1H NMR spectrum of **13a** displayed two singlet signals at δ 3.60, 3.67 ppm due to two methoxy groups and the seven aromatic protons, besides the D_2O exchangeable protons were observed as two singlet signals at δ 10.98, 11.52 ppm. Its mass spectrum showed a molecular ion peak at m/z 349, which is characteristic of the molecular formula $\text{C}_{19}\text{H}_{15}\text{N}_3\text{O}_4$ together with base peak at m/z 111. ^{13}C NMR spectra of compound **13b** exhibited two $\text{C}=\text{N}$ and $\text{C}=\text{O}$ carbons at δ 158.54, 158.83 and 165.51 ppm besides the aromatic protons.

3.2. Biological activity

3.2.1. Anti-proliferative activity and structure activity relationship study

All the newly synthesized compounds were screened for their anticancer activity against three cell lines, which are human breast

cancer cell line (MCF-7), human liver carcinoma (HepG-2), and colon cancer cell line (HCT-116). The entire tested compound showed moderate to high anticancer activity against MCF-7 cells with IC_{50} ranging from 0.68 to 35.60 μM (Table 1). Compounds **2b**, **5**, **8b**, **12** and **13a,b** elicited the highest antitumor activity against the MCF-7 cell lines with IC_{50} 0.76, 2.81, 0.68, 1.28, 2.47 and 2.87 μM respectively compared with the standard Imatinib, which has IC_{50} 6.06 μM . For the HepG-2 cell line, it found that the same compounds **2a**, **2b**, **5**, **6**, **8b**, **12**, **13a** and **13b** were showing the highest activity with IC_{50} 4.73, 2.44, 2.88, 5.33, 2.80, 95, 1.30, 3.02, and 2.95 μM , respectively, in comparison to Imatinib which has IC_{50} 5.50 μM for this cell line.

Also, compounds **2b**, **8b**, and **12** represent the highest activity against HCT-116 cell line in which the IC_{50} was 2.48, 0.74, and 0.76 μM , respectively. Other compounds showed moderate activity against the three cell lines. This series's most active compounds were **8b** containing spiro-pyrazole moiety with IC_{50} 0.74, 0.95, and 0.68 μM compared with the standard Imatinib with IC_{50} 6.06 5.50, and 4.70 μM against the tested cell lines. Also, compound **2b**, which have IC_{50} 0.76, 2.44, and 2.48 μM , indicates that the free acetyl group's presence showed good activity against the cell lines. Upon reaction of compound **2** with hydrazine hydrate or thiosemicarbazide to afford **3a** and **3b**, the activity was diminished, and this may be due to the absence of carbonyl in acetyl group and formed hydrazone derivatives.

Chalcone **4**, which formed through the reaction of **2b** with anisaldehyde, have moderate activity against the three cell lines with IC_{50} 8.91, 11.30, and 24.90 μM against MCF-7, HepG-2, and HCT-116 cell lines respectively, this may be due to the presence of methoxy group which has + *M* effect. On the other hand, 3-hydroxyindolin-2-one derivative **5** showed higher activity against the three cell lines with IC_{50} 2.81, 2.88, and 3.22 μM , which means that the free amino group's presence increases activity. Moreover, when this amino group blocked as in compound **7** through salicylaldehyde reaction, the antitumor activity decreased. Furthermore, in Scheme 2, the most active compounds were **12**, **13a** and **13b** with IC_{50} (1.28, 1.30 and 0.76 μM), (2.47, 3.02, and 5.85 μM) and (2.87, 2.95, and 4.76 μM) respectively and this may be due to the formation of spiro-chromane moiety in compound **12**. The increase of anticancer activity for compounds **13a** and **13b** may be due to the presence of furo[2,3-*b*]indole and carboxamide moieties in addition to isatin moiety.

Finally, it found that the most active compounds contained free acetyl or amino groups in *p*- position, spiro-pyrazole, spiro-chromane, and furo[2,3-*b*]indole carboxamide moieties; this is beside the isatin structure as shown in Table 1.

3.2.2. Apoptosis detection studies

3.2.2.1. Effect on the active caspase-3 level. Caspase-3 is one of the central 'executioners' of apoptosis that stimulates apoptosis by attacking many profitable proteins required by the cell and therefore induced programmed cell death. Caspase-3 consists of two subunits, with 12 and 17-kDa, and each subunit contains three and five thiol functions, respectively [67–69]. Caspase-3 activation for the most promising compounds depending on the IC_{50} results was evaluated to explain the anti-proliferative activity mechanism, and the obtained data are represented in (Fig. 2 and Table 2). Spiro pyrazole derivatives **8b** revealed the best Caspase-3 activator with concentration 537.29 pg/mL with 10.81 folds than un-treated MCF-7 cell 49.71 pg/mL. Further, both spiro-chroman-2,3'-indolin-2-one derivatives **12** and Schiff's base of 4-aminoacetophenone with isatin **2b** causes overexpression to Caspase-3 level (514.63 and 509.47 pg/mL) by 10.35 and 10.25 folds, respectively. Moreover, 3-hydroxy-2-substituted-2-oxindole derivatives **5** demonstrated the level of Caspase-3 by 8.62 folds.

Finally, furo[2,3-*b*]indol-3-carboxamide derivatives **13a,b** displayed the least Caspase-3 activator level by 8.01 and 8.27 folds, respectively. The presence of 4-florophenyl derivative is favored and induced apoptosis by activate caspase 3 proteins with slightly higher than 2,4-dimethyl phenyl derivative at carboxamide group.

3.2.2.2. Study on mitochondrial apoptosis pathway BAX and Bcl-2 proteins. For further evaluation, BAX and Bcl-2 are proteins present in the mitochondria-mediated pathway and play an important role in tumor resistance to chemotherapy, so an increase in BAX expression and decrease in Bcl-2 can induce the apoptotic process and eliminate cancer cells [70,71]. In general, depending on obtained data from Table 2, it found that treatment of MCF-7 cells with the most promising derivatives **2b**, **5**, **8b**, **12**, **13a**, and **13b** displayed an upregulation of pro-apoptotic protein (BAX) and a down-regulation of anti-apoptotic, (Bcl-2) protein. Furthermore, compounds **8b**, **12**, **2b** induced pro-apoptosis with BAX protein values (461.92, 439.15 and 419.71 pg/mL) by (9.76, 9.28 and 8.87 folds), respectively, in comparison to control value (47.32 pg/mL). Additionally, design polynuclear structure as furo[2,3-*b*]indol-3-carboxamide derivatives **13a**, **13b** demonstrated BAX values (328.58 and 365.41 pg/mL) related to substituent on carboxamide moiety. By the same way, all the tested compounds **2b**, **5**, **8b**, **12**, **13a** and **13b** suppress apoptosis with Bcl-2 values (1.95, 2.12, 1.54, 1.75, 2.58 and 2.31pg/mL) respectively, and less than untreated MCF-7 cells 6.16 pg/mL.

Finally, it was reported that the increased ratio of up-regulating BAX expression to down-regulating Bcl-2 expression plays a significant role in the collapse of mitochondrial membrane, then lead to Cyt c release and cell death [72]. By applying BAX/ Bcl-2 ratio to consideration value of the MCF-7 cell, the most active compound **8b** showed ratio nearly to 39 folds as compared to the control, at the same time the other compounds **2b**, **5**, **12**, **13a** and **13b** established to have ratio 27.95, 23.09, 32.60, 16.59 and 20.62 folds respectively.

3.2.3. Flow cytometric analysis and apoptotic studies

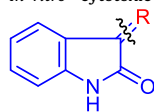
One of the most promising cancer therapy strategies is cell cycle targeting for cell line [73]. In this study compound, **8b** was chosen among the most active compounds for further studies and investigated its molecular mechanism of action.

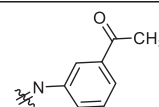
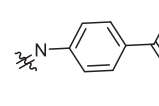
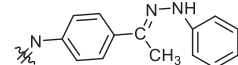
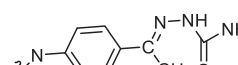
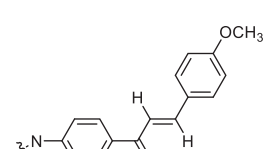
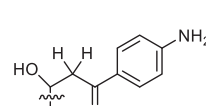
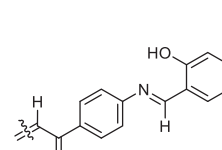
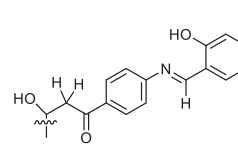
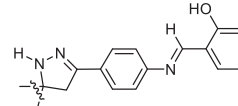
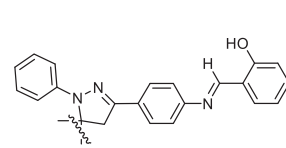
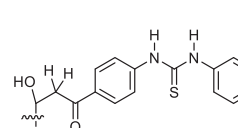
3.2.3.1. Cell cycle analysis. Compound **8b** that have spiroindolie-3,3'-pyrazole derivative on its structure was evaluated cell cycle distribution by flow cytometric analysis in MCF-7 cells, upon treating the cell with ten μM to study its effect on the cell cycle phases. As shown in Fig. 3 and Table 3, the obtained result observed that spiroindolie-3,3'-pyrazole derivative **8b** arrested in G2/M phase by 47.95% and reduced in S phase (29.21%) in comparison to control as well as induced apoptosis at priG1 and G0-G1 phases by 17.36 and 22.84%, respectively.

3.2.3.2. Annexin-V FITC apoptotic study. The apoptotic activity of spiroindoline-3,3'-pyrazole derivative **8b** was measured via flow cytometry detection using Annexin V-FITC and propidium iodide (PI) double staining. As shown in Fig. 5 and Table 4, upon treating the MCF-7 cells by compound **8b**, the results demonstrate a significant increase in the total apoptosis (17.36%) when compared with the control (3.17%). Also, compound **8b** induced apoptosis in the late-stage higher than early stage 8.15, 6.46%. These data represented in Figs. 4 and 5 and Table 4 suggest that compound **8b** is a good apoptotic agent.

3.2.4. In vitro EGFR inhibition assay

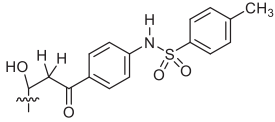
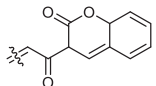
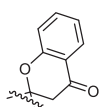
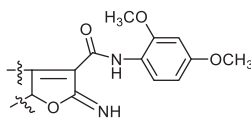
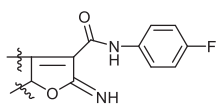
One of the important biomarkers for several different tumor types and an attractive drug target in cancer therapy is the Epidermal Growth Factor Receptor. EGFR (also known as HER1 or erbB-1)

Table 1*In vitro*^a cytotoxic activity of the synthesized compounds and Imatinib against MCF-7, HepG-2, and HCT-116


| Cpd. No. | R | IC ₅₀ μM/mL/SI ^b | | | |
|----------|-------------------------------------------------------------------------------------|----------------------------------------|--------------------|--------------------|---------------|
| | | MCF-7 | HepG-2 | HCT-116 | WI-38 |
| 2a |  | 11.40 ± 0.89 | 4.73 ± 0.34 | 5.80 ± 0.45 | ND |
| 2b |  | 0.003 (250.7) | 2.011 (78) | 2.48 ± 0.12 (78.8) | 190.5 ± 1.87 |
| 3a |  | 35.60 ± 1.6 | 18.60 ± 1.25 | 21.70 ± 1.4 | ND |
| 3b |  | 50 < | 50 < | 50 < | ND |
| 4 |  | 8. ± 0.73 | 11.30 ± 0.90 | 24.90 ± 1.5 | ND |
| 5 |  | 2.81 ± 0.15 (67) | 2.88 ± 0.16 (65.5) | 3.22 ± 0.21 (58.6) | 188.76 ± 1.65 |
| 6 |  | 12.10 ± 0.94 | 5.33 ± 0.45 | 4.50 ± 0.32 | ND |
| 7 |  | 9.82 ± 0.84 | 11.10 ± 0.92 | 24.30 ± 1.5 | ND |
| 8a |  | 50 < | 50 < | 50 < | ND |
| 8b |  | 0.68 ± 0.01 (300.5) | 0.95 ± 0.03 (215) | 0.74 ± 0.02 (276) | 204.36 ± 2.78 |
| 9 |  | 6 ± 0.51 | 7.16 ± 0.70 | 5.21 ± 0.35 | ND |

(continued on next page)

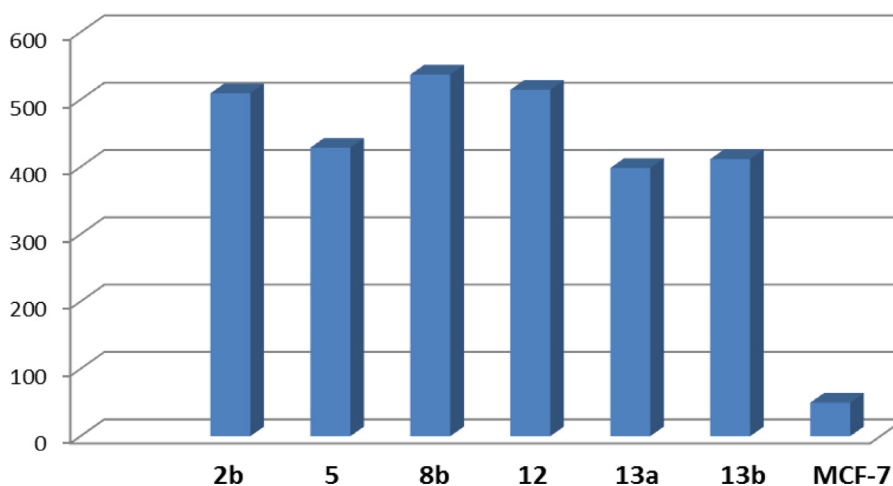
Table 1 (continued)

| Cpd. No. | R | IC ₅₀ μM/mL/SI ^b | | | |
|-----------------|-----------------------------------------------------------------------------------|----------------------------------------|----------------------|----------------------|---------------|
| | | MCF-7 | HepG-2 | HCT-116 | WI-38 |
| 10 |  | 8.76 ± 0.76 | 10.18 ± 0.84 | 13.10 ± 0.95 | ND |
| 11 |  | 21.20 ± 1.3 | 22.40 ± 1.4 | 19.20 ± 1.2 | ND |
| 12 |  | 1.28 ± 0.06 (157.9) | 1.30 ± 0.07 (155) | 0.76 ± 0.02 (265) | 202.08 ± 2.11 |
| 13a |  | 2.47 ± 0.17 (67) | 3.02 ± 0.2 (55) | 5.85 ± 0.39 (28) | 165.98 ± 0.98 |
| 13b |  | 2.87 ± 0.14 (65) | 2.95 ± 0.18 (63) | 4.76 ± 0.35 (39) | 186.55 ± 1.34 |
| Imatinib | | 6 ± 0.51 | 5.50 ± 0.44 | 4.70 ± 0.37 | ND |

ND: Not determined.

^a Data represent the mean values of three independent determinations.^b SI: Selectivity index = (IC₅₀ of WI-38) / (IC₅₀ of cancer cell line).

Caspase-3

**Fig. 2.** A diagram indicating the effect of the most active compounds (**2b**, **5**, **8b**, **12**, **13a**, and **13b**) on apoptotic induction of Caspase-3.

that can be defined as an intracellular signal translation receptor that regulates pathway of proliferation, appointment, angiogenesis, adhesion, and motility of intracellular signal inside the cell and therefore many drug therapy was approved by FDA that use this receptor as a specific target [74–77].

The most promising spiroindoline-3,3'-pyrazole derivative **8b** was evaluated for two types of EGFR enzymatic activity assays us-

ing MCF-7 cells **Table (5)**. Compound **8b** showed inhibitory concentration for EGFR^{WT} with IC₅₀ = 0.014 μM in comparison to Lapatinib (IC₅₀ = 0.025 μM) and Erlotinib (IC₂₀ = 0.065 μM) with nearly two and six folds higher than the positive control, respectively. While in the case of mutant EGFR^{L858R-TK} compound **8b** displayed IC₅₀ value 12.66 nM with 2.82, 4.72 folds greater than reference drugs, Lapatinib and Erlotinib, respectively **Table 5**.

Cell cycle analysis

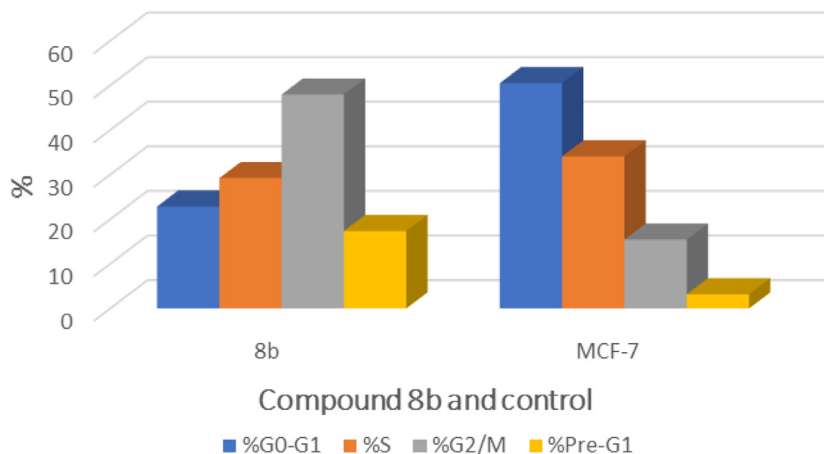
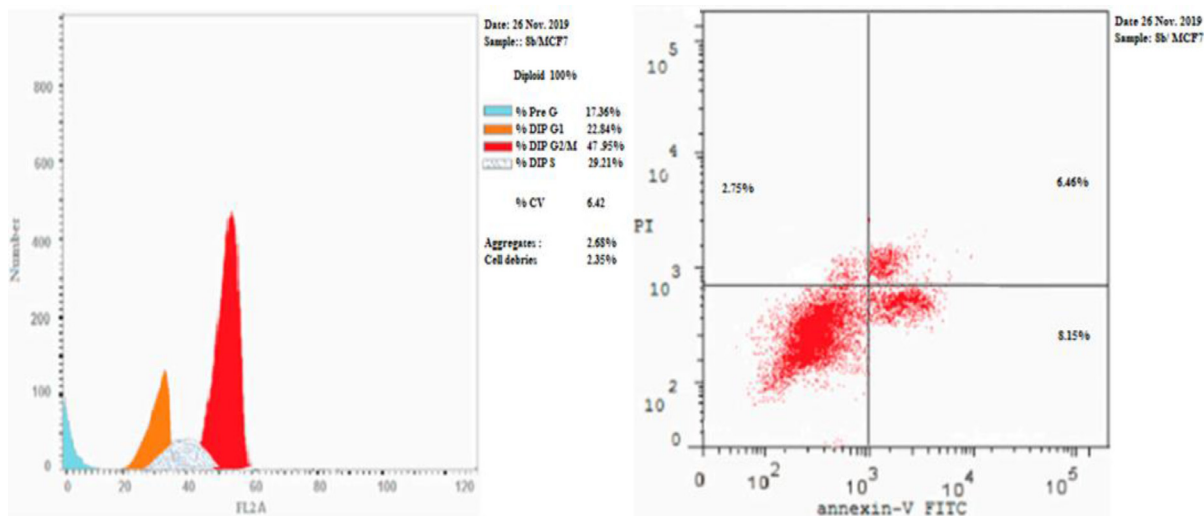
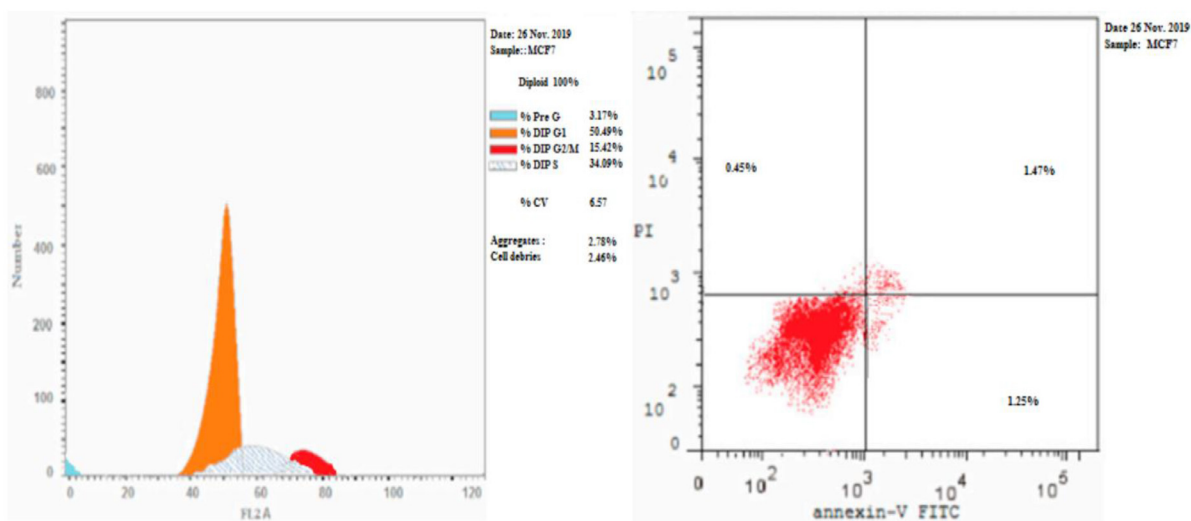


Fig. 3. Cell cycle analysis and apoptosis effect of the most potent compound **8b** on MCF-7 cell line.



i- 8b/ MCF-7



ii- control MCF-7

Fig. 4. Cell cycle and flow cytometer analysis: i- **8b**/ MCF-7 and ii- control MCF-7.

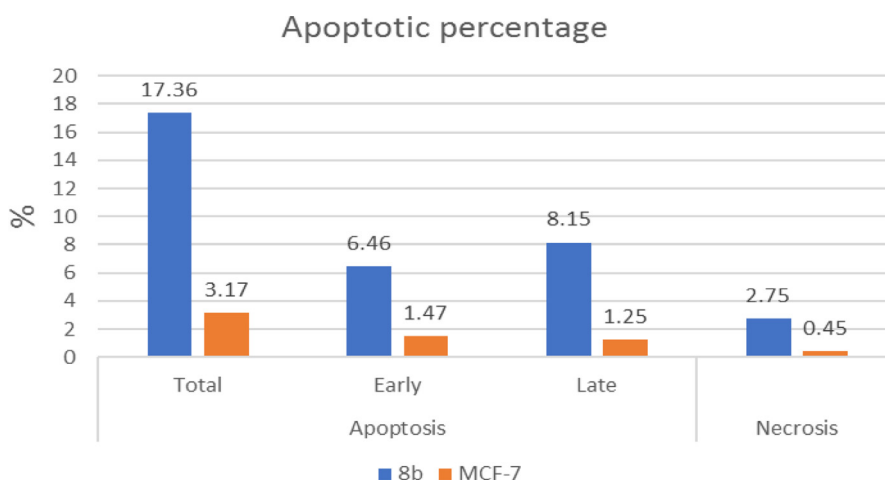


Fig. 5. Diagram illustrates the effect of the compound **8b** on cell death percentage.

3.2.5. In silico computational analysis studies

3.2.5.1. In silico evaluation of physicochemical and ADME properties.

Computational testing was performed to evaluate physical and ADME properties of the most biologically active synthesized compounds (**2b**, **5**, **8b**, **12**, **13a**, and **13b**, in addition to Imatinib and Erlotinib). Both synthesized compounds are in no way in violation of the Lipinski rule for oral drugs for their physical-chemical characteristics (Table 6). Therefore, all hits follow the drug-like re-

Table 2

Effect of most promising compounds (**2b**, **5**, **8b**, **12**, **13a**, and **13b**) on the gene's expression and apoptosis markers.

| Cpd. No. | Caspase-3 Pg/mL (Fold) | BAX Pg/mL(Fold) | Bcl-2 Pg/mL (Fold) | BAX/Bcl-2 ratio |
|--------------|------------------------|-----------------|--------------------|-----------------|
| 2b | 509.47 (10.25) | 419.71 (8.87) | 1.95 (3.15) | 27.95 |
| 5 | 428.72 (8.62) | 375.64 (7.94) | 2.12 (2.86) | 23.09 |
| 8b | 537.29 (10.81) | 461.92 (9.76) | 1.54 (3.99) | 38.98 |
| 12 | 514.63 (10.35) | 439.15 (9.28) | 1.75 (3.51) | 32.60 |
| 13a | 398.43 (8.01) | 328.58 (6.94) | 2.58 (2.39) | 16.59 |
| 13b | 411.55 (8.28) | 365.41 (7.72) | 2.31 (2.67) | 20.62 |
| MCF-7 | 49.71 | 47.32 | 6.16 | 1 |

Table 3

Results of cell cycle analysis in MCF-7 expressed by (%) of cells in each phase when treated with **8b**.

| Cpd. No. | %G0-G1 | %S | %G2/M | %Pre-G1 |
|--------------|--------|-------|-------|---------|
| 8b | 22.84 | 29.21 | 47.95 | 17.36 |
| MCF-7 | 50.49 | 34.09 | 15.42 | 3.17 |

Table 4

Different Percent of cell death induced by compounds **8b** on MCF-7 cells.

| Cpd. No. | Apoptosis | | | Necrosis |
|--------------|-----------|-------|------|----------|
| | Total | Early | Late | |
| 8b | 17.36 | 6.46 | 8.15 | 2.75 |
| MCF-7 | 3.17 | 1.47 | 1.25 | 0.45 |

Table 5

IC₅₀ of the representative anticancer active compound **8b** on EGFR in MCF-7 cells.

| Cpd. No. | Enzyme inhibitory activity IC ₅₀ | |
|------------------|---------------------------------------------|-------------------------------|
| | EGFR ^{WT} (μM) | EGFR ^{L858R-TK} (nM) |
| 8b | 0.014 | 12.66 |
| Lapatinib | 0.025 | 35.72 |
| Erlotinib | 0.0653 | 59.72 |

quirements in the screening process according to Veber's rules. Both compounds have rotary bonds from 2 to 10 that demonstrate molecular stability against their bio-targets, except compound **12**, which has zero rotary bonds.

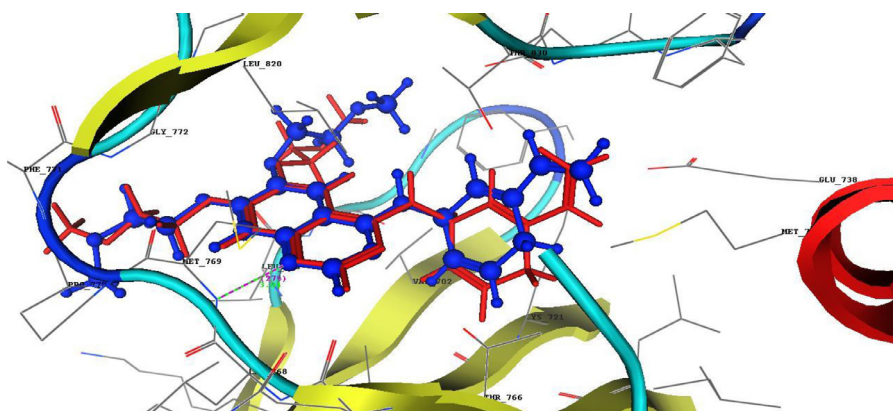
The total topological polar area (TPSA) (Table 6) is higher than 55.40 °Å². The absorption (percent of ABS) was further estimated by using the equation percentage ABS % = 109 - (0.345 x TPSA) [78] and found that the calculated percent ABS of all these hits varied between 76.92 and 89.89 %, which showed that the cell membrane permeability and bioavailability of such synthesized derivatives were required.

In relation to parameters of pharmacokinetic and some medicinal chemistry parameters for the newly synthesized compounds, it was observed that all tested compounds with good gastrointestinal absorption and no blood-brain barrier permeation, except **2b**, **12**, and **13b**, which can pass the blood-brain barrier and can cause CNS side effects. (Table 7)

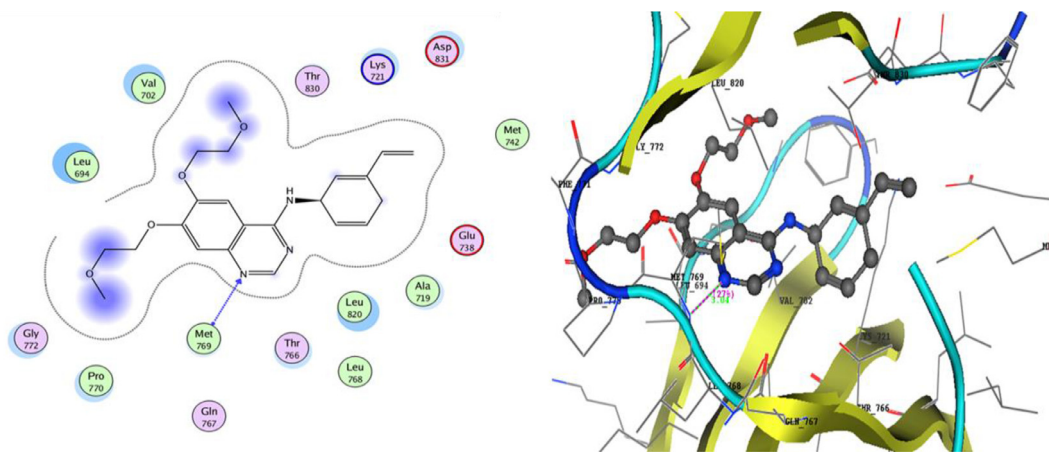
Another significant factor throughout the preclinical research review was the examination of a non-substrate P-glycoprotein (P-gp) candidature. P-gp acts as an effluent transport mechanism that pumps medicines and other compounds out of the cell and its substrate is one of the factors behind its resistance to cancer chemotherapy. P-gp was found to be a vital carrier of the medicament, thus resisting drugs such as Imatinib [79]. Thus, our compounds were analyzed on the website of SwissADME (<http://swissadme.ch/index.php>), and most of the hits are not P-gp protein substrates, as seen in Table 7. It indicates that **2b**, **8b** and **13a**, have very little chance of effluxing out of the cell, leading to full impact.

Bioavailability is a plasma quantity index and is seen as the most important factor affecting absorption. It is important to note the high bioavailability levels of 0.55 of all active synthesized derivatives. SwissADME [47,60] has shown zero hit warnings for pan-assay interference compounds (PAINS). PAINS, while important features must be taken into consideration when designing medicines for the avoidance of false-positive effects, will lead only to the exclusion of promising hits based on fantastic PAINS [80]. All analogs were found to have synthetic accessibility between 2.58 and 4.72 values, suggesting that they can be easily synthesized on a large basis (Table 7).

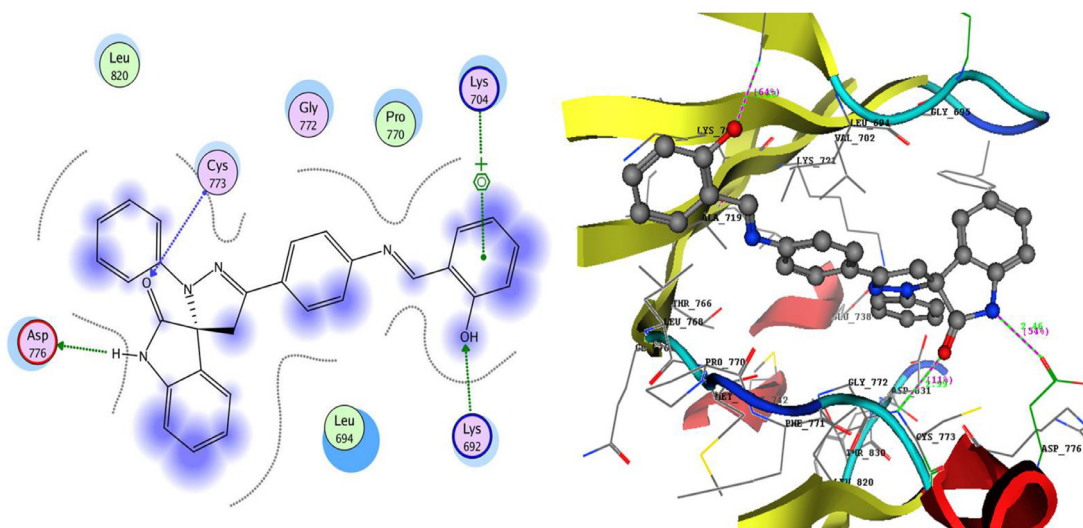
3.2.5.2. Molecular docking studies. In recent years, the computer docking technique plays a major role in drug design by placing a molecule into the binding site of the target enzyme in a non-covalent fashion, and therefore these models provide a more accurate picture of the biologically active molecules at the atomic level



a: Superimposition 3D of the co-crystallized (red) and the docking pose (blue) of Erlotinib with RMSD of 1.10 Å in the active site of 1M17



b: 3D interactions of Erlotinib in the active site of 1M17



c: 2D & 3D interaction maps of compound 8b inside 1M17 active site

Fig. 6a. Superimposition 3D of the co-crystallized (red) and the docking pose (blue) of Erlotinib with RMSD of 1.10 Å in the active site of 1M17. **Fig. 6b:** 3D interactions of Erlotinib in the active site of 1M17. **Fig. 6c:** 2D & 3D interaction maps of compound 8b inside 1M17 active site.

Table 6
Physicochemical properties based on Lipinski's rule of five, Veber's rule, TPSA, and% ABS.

| Cpd. no. | HBD < 5 | HBA < 10 | MlogP < 4.15 | MW < 500 | RT* | TPSA* °A ² | ABS % | Lipinski's Violations | Veber's violations |
|------------------|---------|----------|--------------|----------|-----|-----------------------|-------|-----------------------|--------------------|
| 2b | 1 | 3 | 1.5 | 264.28 | 2 | 58.53 | 88.81 | 0 | 0 |
| 5 | 3 | 3 | 0.75 | 282.29 | 3 | 92.42 | 77.12 | 0 | 0 |
| 8b | 2 | 4 | 3.60 | 458.51 | 4 | 77.29 | 82.33 | 0 | 0 |
| 12 | 1 | 3 | 1.58 | 265.26 | 0 | 55.40 | 89.89 | 0 | 0 |
| 13a | 2 | 6 | 1.46 | 349.34 | 5 | 93.00 | 76.92 | 0 | 0 |
| 13b | 2 | 5 | 2.45 | 307.28 | 3 | 74.54 | 83.28 | 0 | 0 |
| Imatinib | 2 | 6 | 2.15 | 493.60 | 8 | 86.28 | 79.23 | 0 | 0 |
| Erlotinib | 1 | 6 | 1.62 | 393.44 | 10 | 74.73 | 83.22 | 0 | 0 |

*RT= rotatable bond, TPSA =topological polar surface area,.

Table 7
Pharmacokinetic properties and medicinal chemistry parameters.

| Cpd. no. | GI Absorption | BBB Permeation | Pgp substrate | Bioavailability Score | PAINS Alerts | Synthetic Accessibility |
|------------------|---------------|----------------|---------------|-----------------------|--------------|-------------------------|
| 2b | High | Yes | No | 0.55 | 0 | 2.59 |
| 5 | High | No | Yes | 0.55 | 0 | 2.58 |
| 8b | High | No | No | 0.55 | 0 | 4.72 |
| 12 | High | Yes | Yes | 0.55 | 0 | 3.38 |
| 13a | High | No | No | 0.55 | 0 | 3.65 |
| 13b | High | Yes | Yes | 0.55 | 0 | 3.38 |
| Imatinib | High | No | Yes | 0.55 | 0 | 3.78 |
| Erlotinib | High | Yes | No | 0.55 | 0 | 3.19 |

[81]. In order to have an insight into the molecular interaction of most potent compound **8b** with epidermal growth factor receptor kinase domain (EGFR), the docking study was performed to explore the mode of interactions of compound **8b** with amino acids in the active site of the enzyme (PDB ID **1M17**) [24], that was downloaded from protein data bank (www.rcsb.org) as crystal structure and co-crystallized with Erlotinib inhibitor (4-anilinoquinazoline). Redocking process of co-crystallized ligand observed docking score $S = -17.84$ kcal/mol, and RMSD of 1.10 °A with only one hydrogen bond with Met 769 and nitrogen of quinazoline with bond length (3.04 °A) (Fig. 6a,b). Molecular modeling was carried out using Molecular Operating Environment software 10.2008 (MOE), Chemical Computing Group Inc., Montreal, Quebec, Canada, the docking results were achieved, and the best confirmation model with the high docking score was investigated for analysis.

Compound **8b** admitted a lower docking score energy (-18.76 kcal/mol), with two hydrogen bonds acceptor, one hydrogen bond bonded between Cys773 with the carbonyl of isatin with bond length (2.99 °A) with a strength of 11 %, and another one between Lys692 and hydroxy group of salicylaldehyde derivative with bond length (2.63 °A) and strength of 64 %. Also, there is one H-bond sidechain donor between NH of isatin derivative and Asp776 with bond length 2.46 °A and strength (54%) and an arene-cation interaction observed between Lys 704 and phenyl group of salicylaldehyde derivative (Figure 6c).

Our synthetic strategy in this research involves three chiral compounds as **8a**, **8b**, and **12**. However, only one derivative **8b** showed good anti-proliferative activity with lower IC₅₀ values against EGFR expression; for the previous reason, further docking study for both derivatives **8b** and **12** was performed to illustrate this conflict. Docking of Compound **8a** displayed binding energy $S = -14.52$ kcal/mol, with only one hydrogen bond between the nitrogen of pyrazole and Cys773 with bond length 3.15 °A and strength 13%. Furthermore, Compound **12** exhibited binding energy $S = -12.72$ kcal/mol, with two hydrogen bonds between the carbonyl of chromone and isatin with the residues Lys721 and Thr766 with bond length 3.10°A 2.67°A respectively (See supplementary material). Finally, it can be concluded that spiro indoline-3,3'-pyrazole derivative **8b** could enhance anti-proliferative activity with EGFR inhibition by lower binding energy (-18.76) and

different interaction as hydrogen bond (three bonds), arene-cation, and hydrophobic interactions.

4. Conclusions

A new series of isatin-linked chalcones and Schiff's base in this work were synthesized and evaluated as novel apoptotic agents. The target compounds were examined for their cytotoxic activity against three human cell lines, which are breast cancer cell lines (MCF-7), liver hepatocellular carcinoma (HepG-2), and colon carcinoma cell lines (HCT-116). Compounds **2b**, **5**, **8b**, **12**, **13a**, and **13b** displayed to be the most potent in this study compared to Imatinib as the reference standard drug. Compound **8b** was found to be the most potent against the three cell lines. Furthermore, apoptotic studies conducted by these active compounds revealing that apoptosis was accomplished by up-regulation of BAX and Caspase-3 and down-regulation of Bcl-2. Moreover, **8b**, the most potent compound tested for their activity on the cell cycle MCF-7, revealed that they arrest cells at G2/M phase in the cell cycle. Also, the inhibitory activity for compound **8b** against wild EGFR^{WT} and mutant EGFR^{L858R-TK} were done. It showed IC₅₀= 0.014 μM in comparison to Lapatinib (IC₅₀= 0.025 μM) and Erlotinib (IC₂₀= 0.065 μM), while in the case of mutant EGFR^{L858R-TK} **8b** displayed IC₅₀ value 12.66 nM with 2.82, 4.72 folds greater than reference drugs, Lapatinib and Erlotinib, respectively. Physicochemical and ADME properties are also done for the most active compounds as well as docking simulation for compound **8b**. Finally, depending on the above studies, we can conclude that among the most active compounds, only one compound (spiroindoline-3,3'-pyrazole derivative) **8b** was selected for further studies to elucidate the mechanism of cell death and therefore, the advanced studies displayed that compound **8b** capable of inducing apoptosis by multiple mechanisms, which helps us in the future work for this structure.

Declaration of Competing Interest

The authors declare that they have no known competing financial interests or personal relationships that could have appeared to influence the work reported in this paper. The authors declare the

following financial interests/personal relationships which may be considered as potential competing interests.

Supplementary materials

Supplementary material associated with this article can be found, in the online version, at [doi:10.1016/j.molstruc.2021.130159](https://doi.org/10.1016/j.molstruc.2021.130159).

CRedit authorship contribution statement

Eman A. Fayed: Conceptualization, Methodology, Validation, Formal analysis, Investigation, Resources, Writing - original draft, Writing - review & editing, Visualization. **Rogy R. Ezz Eldin:** Methodology, Visualization. **Ahmed B.M. Mehany:** Validation, Formal analysis, Writing - original draft, Writing - review & editing. **Ashraf H. Bayoumi:** Supervision, Writing - review & editing. **Yousry A. Ammar:** Conceptualization, Validation, Formal analysis, Resources, Writing - original draft, Writing - review & editing.

Reference

- [1] R. Siegel, J. Ma, Z. Zou, A. Jemal, Cancer statistics, 2014, CA. Cancer J. Clin. 64 (2014) 9–29, doi:[10.3322/caac.21208](https://doi.org/10.3322/caac.21208).
- [2] B.N. Ames, L.S. Gold, Endogenous mutagens and the causes of aging and cancer, Mutat. Res. Mol. Mech. Mutagen. 250 (1991) 3–16, doi:[10.1016/0027-5107\(91\)90157-J](https://doi.org/10.1016/0027-5107(91)90157-J).
- [3] B.R. Vijay Avin, P. Thirusangu, V. Lakshmi Ranganatha, A. Firdouse, B.T. Prabhakar, S.A. Khanum, Synthesis and tumor inhibitory activity of novel coumarin analogs targeting angiogenesis and apoptosis, Eur. J. Med. Chem. 75 (2014) 211–221, doi:[10.1016/j.ejmech.2014.01.050](https://doi.org/10.1016/j.ejmech.2014.01.050).
- [4] T. Nasr, S. Bondock, M. Youns, Anticancer activity of new coumarin substituted hydrazide-hydrazone derivatives, Eur. J. Med. Chem. 76 (2014) 539–548, doi:[10.1016/j.ejmech.2014.02.026](https://doi.org/10.1016/j.ejmech.2014.02.026).
- [5] N. Jiang, X. Zhai, Y. Zhao, Y. Liu, B. Qi, H. Tao, P. Gong, Synthesis and biological evaluation of novel 2-(2-arylmethylene)hydrazinyl-4-aminoquinazoline derivatives as potent antitumor agents, Eur. J. Med. Chem. 54 (2012) 534–541, doi:[10.1016/j.ejmech.2012.05.039](https://doi.org/10.1016/j.ejmech.2012.05.039).
- [6] E.A. Fayed, Y.A. Ammar, A. Ragab, N.A. Gohar, A.B.M. Mehany, A.M. Farag, In vitro cytotoxic activity of thiazole-indenoquinoline hybrids as apoptotic agents, design, synthesis, physicochemical and pharmacokinetic studies, Bioorg. Chem. 100 (2020) 103951, doi:[10.1016/j.bioorg.2020.103951](https://doi.org/10.1016/j.bioorg.2020.103951).
- [7] C. Wang, R.J. Youle, The role of mitochondria in apoptosis*, Annu. Rev. Genet. 43 (2009) 95–118, doi:[10.1146/annurev-genet-102108-134850](https://doi.org/10.1146/annurev-genet-102108-134850).
- [8] L. Galluzzi, O. Kepp, G. Kroemer, 5 - pathophysiology of cancer cell death, in: J.E. Niederhuber, J.O. Armitage, J.H. Doroshow, M.B. Kastan (Eds.), Content Repository Only, Philadelphia, 2014, pp. 69–77.e3, doi:[10.1016/B978-1-4557-2865-7.00005-9](https://doi.org/10.1016/B978-1-4557-2865-7.00005-9).
- [9] G. Xu, Y. Shi, Apoptosis signaling pathways and lymphocyte homeostasis, Cell Res. 17 (2007) 759–771, doi:[10.1038/cr.2007.52](https://doi.org/10.1038/cr.2007.52).
- [10] J. Lopez, S.W.G. Tait, Mitochondrial apoptosis: killing cancer using the enemy within, Br. J. Cancer. 112 (2015) 957–962, doi:[10.1038/bjc.2015.85](https://doi.org/10.1038/bjc.2015.85).
- [11] S. Elmore, Apoptosis: a review of programmed cell death, Toxicol. Pathol. 35 (2007) 495–516, doi:[10.1080/01926230701320337](https://doi.org/10.1080/01926230701320337).
- [12] O. Julien, J.A. Wells, Caspases and their substrates, Cell Death Differ 24 (2017) 1380–1389, doi:[10.1038/cdd.2017.44](https://doi.org/10.1038/cdd.2017.44).
- [13] X.-H. Yang, T.L. Sladek, X. Liu, B.R. Butler, C.J. Froelich, A.D. Thor, Reconstitution of caspase 3 sensitizes MCF-7 breast cancer cells to doxorubicin and etoposide-induced apoptosis, Cancer Res. 61 (2001) 3481P–3435A <http://cancerres.aacrjournals.org/content/61/1/3481.abstract>.
- [14] A. Saraste, K. Pulkki, Morphologic and biochemical hallmarks of apoptosis, Cardiovasc. Res. 45 (2000) 528–537, doi:[10.1016/S0008-6363\(99\)00384-3](https://doi.org/10.1016/S0008-6363(99)00384-3).
- [15] R.C. Taylor, S.P. Cullen, S.J. Martin, Apoptosis: controlled demolition at the cellular level, Nat. Rev. Mol. Cell Biol. 9 (2008) 231–241, doi:[10.1038/nrm2312](https://doi.org/10.1038/nrm2312).
- [16] A.B. Parrish, C.D. Freil, S. Kornbluth, Cellular mechanisms controlling caspase activation and function, Cold Spring Harb. Perspect. Biol. 5 (2013) a008672, doi:[10.1101/cshperspect.a008672](https://doi.org/10.1101/cshperspect.a008672).
- [17] M. Woo, R. Hakem, M.S. Soengas, G.S. Duncan, A. Shahinian, D. Kägi, A. Hakem, M. McCurach, W. Khoo, S.A. Kaufman, G. Senaldi, T. Howard, S.W. Lowe, T.W. Mak, Essential contribution of caspase 3/ CPP32 to apoptosis and its associated nuclear changes, Genes Dev 12 (1998) 806–819, doi:[10.1101/gad.12.6.806](https://doi.org/10.1101/gad.12.6.806).
- [18] G. Pistritto, D. Trisciuglio, C. Ceci, A. Garufi, G. D'Orazi, Apoptosis as anti-cancer mechanism: function and dysfunction of its modulators and targeted therapeutic strategies, Age. (Albany, NY). 8 (2016) 603–619, doi:[10.18632/aging.100934](https://doi.org/10.18632/aging.100934).
- [19] A. Gupta, S. Nigam, I. Avasthi, B. Sharma, B. Ateeq, S. Verma, Caspase-3 mediated programmed cell death by a gold-stabilised peptide carbene, Bioorg. Med. Chem. Lett. 29 (2019) 126672, doi:[10.1016/j.bmcl.2019.126672](https://doi.org/10.1016/j.bmcl.2019.126672).
- [20] B.Q. Tran, S. Jung, Modulation of chloroplast components and defense responses during programmed cell death in tobacco infected with pseudomonas syringae, Biochem. Biophys. Res. Commun. 528 (2020) 753–759, doi:[10.1016/j.bbrc.2020.05.086](https://doi.org/10.1016/j.bbrc.2020.05.086).
- [21] A.R.D. Delbridge, S. Grabow, A. Strasser, D.L. Vaux, Thirty years of BCL-2: translating cell death discoveries into novel cancer therapies, Nat. Rev. Cancer. 16 (2016) 99.
- [22] D. Singh, B.K. Attri, R.K. Gill, J. Bariwal, Review on EGFR inhibitors: critical updates, Mini Rev. Med. Chem. 16 (2016) 1134–1166.
- [23] A.M.S. El-sharief, Y.A. Ammar, A. Belal, M.A.M.S. El-sharief, Y.A. Mohamed, A.B.M. Mehany, G.A.M. Elhag, A. Ragab, Design, synthesis, molecular docking and biological activity evaluation of some novel indole derivatives as potent anticancer active agents and apoptosis inducers, Bioorg. Chem. 85 (2019) 399–412, doi:[10.1016/j.bioorg.2019.01.016](https://doi.org/10.1016/j.bioorg.2019.01.016).
- [24] A.R.Y.A. Ammar, A.M. Sh. El-Sharief, A. Belal, S.Y. Abbas, Y.A. Mohamed, A.B.M. Mehany, Design, synthesis, antiproliferative activity, molecular docking and cell cycle analysis of some novel (morpholinisulfonyl) isatins with potential EGFR inhibitory activity, Eur. J. Med. Chem. 156 (2018) 918–932, doi:[10.1016/j.ejmech.2018.06.061](https://doi.org/10.1016/j.ejmech.2018.06.061).
- [25] C. Unger, New therapeutic approaches in cancer treatment, Drugs Future 22 (1997) 1337–1345.
- [26] V.R. Solomon, C. Hu, H. Lee, Hybrid pharmacophore design and synthesis of isatin-benzothiazole analogs for their anti-breast cancer activity, Bioorg. Med. Chem. 17 (2009) 7585–7592, doi:[10.1016/j.bmc.2009.08.068](https://doi.org/10.1016/j.bmc.2009.08.068).
- [27] M.F. Ullah, M.W. Khan, Food as medicine: potential therapeutic tendencies of plant derived polyphenolic compounds, Asian Pac J Cancer Prev 9 (2008) 187–196.
- [28] G.S. Singh, Z.Y. Desta, Isatins as privileged molecules in design and synthesis of spiro-fused cyclic frameworks, Chem. Rev. 112 (2012) 6104–6155, doi:[10.1021/cr300135y](https://doi.org/10.1021/cr300135y).
- [29] B.V. Silva, Isatin, a versatile molecule: studies in Brazil, J. Braz. Chem. Soc. 24 (2013) 707–720.
- [30] P. Pakravan, S. Kashanian, M.M. Khodaei, F.J. Harding, Biochemical and pharmacological characterization of isatin and its derivatives: from structure to activity, Pharmacol. Reports. 65 (2013) 313–335, doi:[10.1016/S1734-1140\(13\)71007-7](https://doi.org/10.1016/S1734-1140(13)71007-7).
- [31] G. Achanta, A. Modzelewska, L. Feng, S.R. Khan, P. Huang, A Boronic-Chalcone derivative exhibits potent anticancer activity through inhibition of the proteasome, Mol. Pharmacol. 70 (2006) 426LP–42433, doi:[10.1124/mol.105.021311](https://doi.org/10.1124/mol.105.021311).
- [32] Y.A. Ammar, E.A. Fayed, A.H. Bayoumi, R.R. Ezz, M.S. Alsaied, A.M. Soliman, M.M. Ghorab, New chalcones bearing isatin scaffold: synthesis, molecular modeling and biological evaluation as anticancer agents, Res. Chem. Intermed. 43 (2017) 6765–6786, doi:[10.1007/s11164-017-3019-z](https://doi.org/10.1007/s11164-017-3019-z).
- [33] Y. Han, W. Dong, Q. Guo, X. Li, L. Huang, The importance of indole and azaindole scaffold in the development of antitumor agents, Eur. J. Med. Chem. (2020) 112506, doi:[10.1016/j.ejmech.2020.112506](https://doi.org/10.1016/j.ejmech.2020.112506).
- [34] A.M. Krause-Heuer, N.R. Howell, L. Matesic, G. Dhand, E.L. Young, L. Burgess, C.D. Jiang, N.A. Lengkeek, C.J.R. Fookes, T.Q. Pham, A new class of fluorinated 5-pyrrolidinylsulfonyl isatin caspase inhibitors for PET imaging of apoptosis, Med. Chem. Comm 4 (2013) 347–352.
- [35] C. Liang, J. Xia, D. Lei, X. Li, Q. Yao, J. Gao, Synthesis, in vitro and in vivo antitumor activity of symmetrical bis-Schiff base derivatives of isatin, Eur. J. Med. Chem. 74 (2014) 742–750, doi:[10.1016/j.ejmech.2013.04.040](https://doi.org/10.1016/j.ejmech.2013.04.040).
- [36] G. Mathur, S. Nain, Recent advancement in synthesis of isatin as anticonvulsant agents: a review, Med. Chem. 4 (2014) 417–427.
- [37] K. Nisha, G. Kumar, K.M. Bhargava, K.-H. Land, R. Chang, S. Arora, V. Sen, N. Kumar, Propargylated isatin-Mannich mono- and bis-adducts: synthesis and preliminary analysis of in vitro activity against Trichomonas foetus, Eur. J. Med. Chem. 74 (2014) 657–663, doi:[10.1016/j.ejmech.2014.01.015](https://doi.org/10.1016/j.ejmech.2014.01.015).
- [38] S.S. Reddy, R. Pallela, D.-M. Kim, M.-S. Won, Y.-B. Shim, Synthesis and evaluation of the cytotoxic activities of some isatin derivatives, Chem. Pharm. Bull. (2013) c13–00400.
- [39] M.C. Rodríguez-Argüelles, R. Cao, A.M. García-Deibe, C. Pelizzi, J. Sanmartín-Matalobos, F. Zani, Antibacterial and antifungal activity of metal(II) complexes of acylhydrazones of 3-isatin and 3-(N-methyl)isatin, Polyhedron. 28 (2009) 2187–2195, doi:[10.1016/j.poly.2008.12.038](https://doi.org/10.1016/j.poly.2008.12.038).
- [40] M.A. Salem, A. Ragab, A.A. Askar, A. El-Khalafawy, A.H. Makhlof, One-pot synthesis and molecular docking of some new spiropyranindol-2-one derivatives as immunomodulatory agents and in vitro antimicrobial potential with DNA gyrase inhibitor, Eur. J. Med. Chem. 188 (2020) 111977, doi:[10.1016/j.ejmech.2019.111977](https://doi.org/10.1016/j.ejmech.2019.111977).
- [41] M.A. Salem, A. Ragab, A. El-Khalafawy, A.H. Makhlof, A.A. Askar, Y.A. Ammar, Design, synthesis, in vitro antimicrobial evaluation and molecular docking studies of indol-2-one tagged with morpholinisulfonyl moiety as DNA gyrase inhibitors, Bioorg. Chem. 96 (2020) 103619, doi:[10.1016/j.bioorg.2020.103619](https://doi.org/10.1016/j.bioorg.2020.103619).
- [42] Y. Zhang, H. Du, H. Liu, Q. He, Z. Xu, Isatin dimers and their biological activities, Arch. Pharm. (Weinheim). 353 (2020) 1900299.
- [43] N.-H. Nam, T.T. Huong, D.T. Mai Dung, P.T. Phuong Dung, D.T. Kim Oanh, D. Quyen, L.T. Thao, S.H. Park, K.R. Kim, B.W. Han, J. Yun, J.S. Kang, Y. Kim, S.-B. Han, Novel isatin-based hydroxamic acids as histone deacetylase inhibitors and antitumor agents, Eur. J. Med. Chem. 70 (2013) 477–486, doi:[10.1016/j.ejmech.2013.10.045](https://doi.org/10.1016/j.ejmech.2013.10.045).
- [44] Z. Xie, G. Wang, J. Wang, M. Chen, Y. Peng, L. Li, B. Deng, S. Chen, W. Li, Synthesis, biological evaluation, and molecular docking studies of novel isatin-thiazole derivatives as α -glucosidase inhibitors, Molecules 22 (2017) 659.

- [45] A.R.Y.A. Ammar, A.M. Sh. El-Sharief, Y.A. Mohamed, A.B.M. Mehany, Synthesis, spectral characterization and pharmacological evaluation of novel thiazole-oxindole hybrid compounds as potent anticancer agent, *Al Zahar Bull. Sci.* 29 (2018) 25–37, doi:[10.21608/ABS.B.2018.33767](https://doi.org/10.21608/ABS.B.2018.33767).
- [46] E.A. Fayed, S.I. Eissa, A.H. Bayoumi, N.A. Gohar, A.B.M. Mehany, Y.A. Ammar, Design, synthesis, cytotoxicity and molecular modeling studies of some novel fluorinated pyrazole-based heterocycles as anticancer and apoptosis-inducing agents, *Mol. Divers.* 23 (2019) 165–181, doi:[10.1007/s11030-018-9865-9](https://doi.org/10.1007/s11030-018-9865-9).
- [47] A.S. Hassan, A.A. Askar, A.M. Naglah, A.A. Almezizia, A. Ragab, Discovery of new Schiff Bases tethered pyrazole moiety: design, synthesis, biological evaluation, and molecular docking study as dual targeting DHFR/DNA gyrase inhibitors with immunomodulatory activity, *Mol.* 25 (2020), doi:[10.3390/molecules25112593](https://doi.org/10.3390/molecules25112593).
- [48] S. ElKalyoubi, E. Fayed, Synthesis and evaluation of antitumour activities of novel fused tri- and tetracyclic uracil derivatives, *J. Chem. Res.* 40 (2016) 771–777, doi:[10.3184/174751916X14798125870610](https://doi.org/10.3184/174751916X14798125870610).
- [49] H.F. Rizk, M.A. El-Borai, A. Ragab, S.A. Ibrahim, Design, synthesis, biological evaluation and molecular docking study based on novel fused pyrazolothiazole scaffold, *J. Iran. Chem. Soc.* 17 (2020) 2493–2505, doi:[10.1007/s13738-020-01944-9](https://doi.org/10.1007/s13738-020-01944-9).
- [50] K. Lahari, R. Sundararajan, Isatin—a potent anti-microbial agent, *Int. J. Res. Pharm. Sci.* 10 (2019) 955–970.
- [51] K.M. Hassan, Z.H. Khalil, Studies on spiroheterocyclic nitrogen compounds, IV synthesis of some new spiro azetidinones and spiro thiazolidinones containing pyrazolines, *Zeitschrift Für Naturforsch. B.* 34 (1979) 1326–1329.
- [52] Y.A. Ammar, E.A. Fayed, A.H. Bayoumi, R.R. Ezz, M.S. Alsaïd, A.M. Soliman, M.M. Ghorab, New chalcones bearing isatin scaffold: synthesis, molecular modeling and biological evaluation as anticancer agents, *Res. Chem. Intermed.* 43 (2017) 6765–6786, doi:[10.1007/s11164-017-3019-z](https://doi.org/10.1007/s11164-017-3019-z).
- [53] S. Lanka, S. Thennarasu, P.T. Perumal, Stoichiometry-controlled cycloaddition of azomethine ylide with dipolarophiles: chemoselective and regioselective synthesis of bis- and tris-spirooxindole derivatives, *Tetrahedron Lett* 55 (2014) 2585–2588, doi:[10.1016/j.tetlet.2014.02.121](https://doi.org/10.1016/j.tetlet.2014.02.121).
- [54] R.A. Kusanur, M. Ghate, M.V. Kulkarni, Synthesis of spiro[indolo-1,5-benzodiazepines] from 3-acetyl coumarins for use as possible anti-anxiety agents, *J. Chem. Sci.* 116 (2004) 265–270, doi:[10.1007/BF02708277](https://doi.org/10.1007/BF02708277).
- [55] A.P. Wilson, Cytotoxicity and viability assays, *Anim. Cell Cult. a Pract. Approach* 3 (2000) 175–219.
- [56] J. Wang, M.J. Lenardo, Roles of caspases in apoptosis, development, and cytokine maturation revealed by homozygous gene deficiencies, *J. Cell Sci.* 113 (2000) 753–757.
- [57] K.K.-W. Lo, T.K.-M. Lee, J.S.-Y. Lau, W.-L. Poon, S.-H. Cheng, Luminescent biological probes derived from ruthenium(II) estradiol poly(pyridine) complexes, *Inorg. Chem.* 47 (2008) 200–208, doi:[10.1021/jc701735q](https://doi.org/10.1021/jc701735q).
- [58] E.A. Fayed, R. Sabour, M.F. Harras, A.B.M. Mehany, Design, synthesis, biological evaluation and molecular modeling of new coumarin derivatives as potent anticancer agents, *Med. Chem. Res.* 28 (2019) 1284–1297, doi:[10.1007/s00044-019-02373-x](https://doi.org/10.1007/s00044-019-02373-x).
- [59] A.R.Y.A. Ammar, A.M. Sh. El-Sharief, A. Belal, S.Y. Abbas, Y.A. Mohamed, A.B.M. Mehany, Design, synthesis, antiproliferative activity, molecular docking and cell cycle analysis of some novel (morpholinosulfonyl) isatins with potential EGFR inhibitory activity, *Eur. J. Med. Chem.* 156 (2018) 918–932, doi:[10.1016/j.ejmech.2018.06.061](https://doi.org/10.1016/j.ejmech.2018.06.061).
- [60] A. Daina, O. Michielin, V. Zoete, SwissADME: a free web tool to evaluate pharmacokinetics, drug-likeness and medicinal chemistry friendliness of small molecules, *Sci. Rep.* 7 (2017) 42717, doi:[10.1038/srep42717](https://doi.org/10.1038/srep42717).
- [61] Y.A. Ammar, A.A. Farag, A.M. Ali, A. Ragab, A.A. Askar, D.M. Elsis, A. Belal, Design, synthesis, antimicrobial activity and molecular docking studies of some novel di-substituted sulfonylquinoxaline derivatives, *Bioorg. Chem.* 104 (2020) 104164, doi:[10.1016/j.bioorg.2020.104164](https://doi.org/10.1016/j.bioorg.2020.104164).
- [62] Y.A. Ammar, A.A. Farag, A.M. Ali, S.A. Hessein, A.A. Askar, E.A. Fayed, D.M. Elsis, A. Ragab, Antimicrobial evaluation of thiadiazino and thiazolo quinoxaline hybrids as potential DNA gyrase inhibitors; design, synthesis, characterization and morphological studies, *Bioorg. Chem.* 99 (2020) 103841, doi:[10.1016/j.bioorg.2020.103841](https://doi.org/10.1016/j.bioorg.2020.103841).
- [63] S.A. El-Kalyoubi, E.A. Fayed, A.S. Abdel-Razek, One pot synthesis, antimicrobial and antioxidant activities of fused uracils: pyrimidodiazepines, lumazines, triazolouracil and xanthines, *Chem. Cent. J.* 11 (2017) 1–13, doi:[10.1186/s13065-017-0294-0](https://doi.org/10.1186/s13065-017-0294-0).
- [64] Y.A.A. Marwa, A.M. Sh. El-Sharief, S.Y. Abbas, M.A. Zahran, Y.A. Mohamed, A. Ragab New 1,3-diaryl-5-thioxo-imidazolidin-2,4-dione derivatives: synthesis, reactions and evaluation of antibacterial and antifungal activities, *Z. Naturforsch.* 71 (2016) 875–881, doi:[10.1515/znB-2016-0054](https://doi.org/10.1515/znB-2016-0054).
- [65] M.M.S. Wassel, A. Ragab, G.A.M. Elhag Ali, A.B.M. Mehany, Y.A. Ammar, Novel adamantane-pyrazole and hydrazone hybridized: design, synthesis, cytotoxic evaluation, SAR study and molecular docking simulation as carbonic anhydrase inhibitors, *J. Mol. Struct.* 1223 (2021) 128966, doi:[10.1016/j.molstruc.2020.128966](https://doi.org/10.1016/j.molstruc.2020.128966).
- [66] S.Y. Abbas, Y.A. Ammar, M.A.M. Sh. El-Sharief, M.M. Ghorab, Y.A. Mohamed, A. Ragab, New imidazolidineiminothione, imidazolidin-2-one and imidazoquinoxaline derivatives: synthesis and evaluation of antibacterial and antifungal activities, *Curr. Org. Synth.* 13 (2016) 466–475.
- [67] H.A. Abou-Zied, B.G.M. Youssif, M.F.A. Mohamed, A.M. Hayallah, M. Abdel-Aziz, EGFR inhibitors and apoptotic inducers: design, synthesis, anticancer activity and docking studies of novel xanthine derivatives carrying chalcone moiety as hybrid molecules, *Bioorg. Chem.* 89 (2019) 102997, doi:[10.1016/j.bioorg.2019.102997](https://doi.org/10.1016/j.bioorg.2019.102997).
- [68] B. Schnurr, T. Ahrens, U. Regenass, 3,27 - optical assays in drug discovery, in: J.B. Taylor, D.J.B.T.-C.M.C.I.I. Triggler (Eds.), Elsevier, Oxford, 2007: pp. 577–598. doi:[10.1016/B0-08-045044-X/00100-0](https://doi.org/10.1016/B0-08-045044-X/00100-0).
- [69] D.A. Stoyanovsky, T.R. Billiar, in: E. Van Faassen, A.B.T.-R. for L. Fyodorovich Vanin (Eds.), Chapter 12 - cellular non-heme iron modulates apoptosis and caspase 3 activity, Elsevier, Amsterdam, 2007, pp. 253–268, doi:[10.1016/B978-0-44452236-8/50012-5](https://doi.org/10.1016/B978-0-44452236-8/50012-5).
- [70] M.H. Ahagh, G. Dehghan, M. Mehdipour, R. Teimuri-Mofrad, E. Payami, N. Sheibani, M. Ghaffari, M. Asadi, Synthesis, characterization, anti-proliferative properties and DNA binding of benzochromene derivatives: increased Bax/Bcl-2 ratio and caspase-dependent apoptosis in colorectal cancer cell line, *Bioorg. Chem.* 93 (2019) 103329, doi:[10.1016/j.bioorg.2019.103329](https://doi.org/10.1016/j.bioorg.2019.103329).
- [71] A. Keskin-Aktan, K.G. Akbulut, Ç. Yazici-Mutlu, G. Sonugur, M. Ocal, H. Akbulut, The effects of melatonin and curcumin on the expression of SIRT2, Bcl-2 and Bax in the hippocampus of adult rats, *Brain Res. Bull.* 137 (2018) 306–310, doi:[10.1016/j.brainresbull.2018.01.006](https://doi.org/10.1016/j.brainresbull.2018.01.006).
- [72] D. Kumar, S. Haldar, M. Gorain, S. Kumar, F.A. Mulani, A.S. Yadav, L. Miele, H.V. Thulasiram, G.C. Kundu, Epoxyazadiradione suppresses breast tumor growth through mitochondrial depolarization and caspase-dependent apoptosis by targeting PI3K/Akt pathway, *BMC Cancer* 18 (2018) 52, doi:[10.1186/s12885-017-3876-2](https://doi.org/10.1186/s12885-017-3876-2).
- [73] B. Yu, S.-Q. Wang, P.-P. Qi, D.-X. Yang, K. Tang, H.-M. Liu, Design and synthesis of isatin/triazole conjugates that induce apoptosis and inhibit migration of MGC-803 cells, *Eur. J. Med. Chem.* 124 (2016) 350–360, doi:[10.1016/j.ejmech.2016.08.065](https://doi.org/10.1016/j.ejmech.2016.08.065).
- [74] Z. Shen, K. Lou, W. Wang, New small-molecule drug design strategies for fighting resistant influenza A, *Acta Pharm. Sin.* B. 5 (2015) 419–430, doi:[10.1016/j.apsb.2015.07.006](https://doi.org/10.1016/j.apsb.2015.07.006).
- [75] H. Masuda, D. Zhang, C. Bartholomeusz, H. Doihara, G.N. Hortobagyi, N.T. Ueno, Role of epidermal growth factor receptor in breast cancer, *Breast Cancer Res. Treat.* 136 (2012) 331–345, doi:[10.1007/s10549-012-2289-9](https://doi.org/10.1007/s10549-012-2289-9).
- [76] P. Cen, C. Walthers, K.W. Finkel, R.J. Amato, Chapter 3 - biomarkers in oncology and nephrology, in: K.W. Finkel, S.C.B.T.-R.D. in C.P. Howard (Eds.), Academic Press, 2014: pp. 21–38. doi:<https://doi.org/10.1016/B978-0-12-415948-8.00003-9>.
- [77] J.L. Hunt, Chapter 9 - immunohistology of head and neck neoplasms, in: D.J.B.T.-D.I. (Third E. Dabbs (Ed.), W.B. Saunders, Philadelphia, 2011: pp. 256–290. doi:<https://doi.org/10.1016/B978-1-4160-5766-6.00013-3>.
- [78] Y.H. Zhao, M.H. Abraham, J. Le, A. Hersey, C.N. Luscombe, G. Beck, B. Sherborne, I. Cooper, Rate-limited steps of human oral absorption and QSAR studies, *Pharm. Res.* 19 (2002) 1446–1457.
- [79] N. Kumar, R. Tomar, A. Pandey, V. Tomar, V.K. Singh, R. Chandra, Preclinical evaluation and molecular docking of 1,3-benzodioxole propargyl ether derivatives as novel inhibitor for combating the histone deacetylase enzyme in cancer, *Artif. Cells, Nanomedicine, Biotechnol* 46 (2018) 1288–1299, doi:[10.1080/21691401.2017.1369423](https://doi.org/10.1080/21691401.2017.1369423).
- [80] S.J. Capuzzi, E.N. Muratov, A. Tropsha, Phantom PAINS: problems with the utility of alerts for pan-assay interference compounds, *J. Chem. Inf. Model.* 57 (2017) 417–427, doi:[10.1021/acs.jcim.6b00465](https://doi.org/10.1021/acs.jcim.6b00465).
- [81] Y.I. El-Gazzar, H.H. Georgey, S.M. El-Messery, H.A. Ewida, G.S. Hassan, M.M. Raafat, M.A. Ewida, H.I. El-Subbagh, Synthesis, biological evaluation and molecular modeling study of new (1,2,4-triazole or 1,3,4-thiadiazole)-methylthio-derivatives of quinoxalin-4(3H)-one as DHFR inhibitors, *Bioorg. Chem.* 72 (2017) 282–292, doi:[10.1016/j.bioorg.2017.04.019](https://doi.org/10.1016/j.bioorg.2017.04.019).